



LUNDS
UNIVERSITET

Storage period optimization of a viscous nasal spray suspension

LTH – Faculty of Engineering

By

Lili Zsófia Domián

Company supervisor:

Jenny Hagelberg

University supervisor:

Marie Wahlgren

2023-05-18

Abstract

The number of people suffering from the unpleasant symptoms of allergic rhinitis is increasing due to environmental and other factors. This not only makes life difficult for the individual but also places a heavy burden on society, which is why treatment is needed. Rhinocort® is a nasal spray suspension manufactured by McNeil AB to reduce the severity of symptoms, and like all medicines, must undergo quality testing. One of these tests is viscosity measurement, which currently is only carried out 6-10 days after production. Therefore, the aim of my thesis was to increase the understanding of the rheology of Rhinocort® and to suggest strategies for shortening the waiting period prior to the viscosity assessment.

A rotational rheometer was used to determine the viscosity of the product. Various methods were set up to evaluate the temperature dependence, recovery, and robustness of the product. In addition, tests were carried out to investigate the influence of different shaking times prior to the measurements. As sedimentation is a recurring phenomenon in the product, this was assessed by amplitude, frequency sweep, and particle size distribution tests. Placebos were also formulated to achieve a higher initial viscosity.

All experiments were successful, as higher viscosity values were achieved by increasing the storage temperature. It was also found that the regeneration of the product after disturbance only takes less than one hour and the suspension itself is incredibly stable. Increasing the shaking time has been shown to have a negative effect on viscosity as it leads to structural destruction. Sedimentation has been shown to start as early as day 0, but this has nothing to do with the overall quality of the product as shown by particle size distribution tests. Additionally, a placebo formulation was done to see if a higher initial viscosity could be achieved by altering the sodium-carboxymethyl-cellulose (NaCMC) content, the excipient responsible for increasing viscosity.

The objectives set with the company were all fulfilled, as the viscosity change was studied in 10 batches between day 0 – day 10 and the above-mentioned tests were performed. I believe that the viscosity testing could be done on day 0 as this value is within specifications. It is important to mention that the goal document submitted to the university portal was based on a preliminary literature search, as it became clear on-site that some experiments are not possible.

Also, as always, there is room for further experiments, and my suggestion would be to examine the viscosity of more batches on day 0 to gather further evidence for my proposal, as I believe that the viscosity test could be done already on this day.

Acknowledgments

This thesis report is the result of long weeks of hard work at McNeil AB, in Helsingborg, and was made possible by the support of the below-mentioned people and many others:

Marie Wahlgren, my university supervisor, professor of the Food Technology Department at Lund University. She has guided me throughout my work and gave me many valuable advice.

Jenny Hagelberg, my company supervisor, Analytical Chemist from the Quality Control Department at McNeil AB. I would like to thank all her support and kindness during my everyday work at the company.

I would like to express my gratitude to the Quality Director at McNeil AB, **Pär Lantz** for providing me with this excellent opportunity. Furthermore, special thanks to my examiner, **Jenny Schelin**, without whom this collaboration would not have been possible.

Finally, many thanks to all the **amazing people at McNeil AB**, who helped me throughout my work, without their contributions this work would not have been finished. They gave support in every step of the experimental process, created a wonderful work environment, and educated me about the different measurements, for which I am incredibly grateful.

Popular science summary

The focus of my thesis work was Rhinocort®, which is a nasal spray for allergy treatment, which is a highly abundant disease and is often undertreated, thus can lead to missed school, - or workdays. Rhinocort® must be tested before it is marketed to ensure good quality and patient safety; one of these tests includes measuring its viscosity. The viscosity value must be within a certain acceptance limit for the product to be marketable, which is 5.0 - 8.5 mPas.

Viscosity can be best understood as the resistance to flow; when we compare the flow properties of honey and water, we can conclude that honey is more viscous as it is much harder to pour out of the jar. Rhinocort® has a so-called thixotropic behaviour, which was assessed throughout some experiments. A thixotropic material becomes less viscous as the force applied to it increases, and this also depends on how long it is exposed to this force.

According to the current test method, 10 days must pass by after production before viscosity tests can be carried out, which leads to high storage costs and hinders production. Therefore, my thesis aimed to shorten this period to save resources and money. Together seven different types of experiments were executed.

For examining the temperature dependence and shaking time dependence, some scientific articles served as the basis, as these suggested an increase in viscosity by lowering the temperature and shortening the time of disturbance (shaking). The product's flow behaviour and its resistance toward mechanical interferences were assessed by various tests, as well as the re-occurring problem, called sedimentation. Furthermore, placebos (the product without the active pharmaceutical ingredient) were mixed to experiment with achieving a higher initial viscosity value.

Table of Contents

1. Introduction	7
1.1 Aim	7
1.2 Description of the product	7
2. Background	8
2.1 Biological background - allergy	8
2.1.1 Process of allergic sensitization	9
2.1.2 Treatment	9
2.1.3 Delivery to the nasal cavity	10
2.2 Suspensions	11
3. Rheology and fluid behaviour	13
3.1 Newtonian behaviour	13
3.2 Non-Newtonian behaviour	15
3.2.1 Shear-thinning and shear-thickening behaviour	15
3.2.2 Thixotropic and rheopectic behaviour	16
3.2.3 Excipients with thixotropic behaviour	16
3.2.4 Other excipients in the nasal suspension	18
4. Methodology	19
4.1 Rheometer and RheoCompass	19
4.1.1 Three-interval loop test	19
4.1.2 Hysteresis loop	20
4.1.3 Amplitude sweep	21
4.1.4 Frequency sweep	21
4.2 Particle size distribution	22
4.3 Placebo formulation	24
5. Results	25
5.1 Investigation of temperature dependent viscosity	28
5.2 The influence of different shaking periods	29
5.3 Test for thixotropic recovery	30
5.4 Frequency sweep and amplitude sweep	31
5.5 High shear rate	32
5.6 Particle size distribution	33
5.7 Placebo testing	36
6. Discussion	38
6.1 Investigation of temperature dependent viscosity	38
6.2 The influence of different shaking periods	39
6.3 Test for thixotropic recovery	39
6.4 Frequency sweep and amplitude sweep	39
6.5 High shear rate	40

6.6	Particle size distribution	41
6.7	Placebo testing	41
7.	Conclusion	43
8.	Future work	45
9.	References	46
10.	Appendix	51
10.1	Temperature dependent viscosity	51
10.2	Viscosity as the function of various shaking times	55
10.3	Thixotropic recovery	57
10.4	Frequency sweep.....	58
10.5	High shear	59

1. Introduction

The product of interest was Rhinocort®, a nasal spray suspension containing budesonide as the active pharmaceutical ingredient (API) for the treatment of allergic rhinitis. This nasal spray aims to ease the unpleasant symptoms of allergy, but before getting the product out to the market it must undergo some quality control tests.

These tests include uniformity of content, weighing, and testing of pH and viscosity, but the latter mentioned measurement is only carried out if the product is left to rest for 6-10 days after manufacture. Needless to say, this hinders the quality control work and shipping of the product, and results in high storage costs.

1.1 Aim

The aim of my thesis was the elimination of this problem by gaining knowledge about the product, its viscosity, and the different influencing factors, such as the temperature and the excipients used.

In order to shorten the maturation period, the temperature dependence of Rhinocort® was inspected and placebos were produced to propose a formulation with higher viscosity values. Furthermore, to improve the measured viscosity values, the shaking time (before measuring) of the product was tested; and to demonstrate the resistance of the product towards strong mechanical forces, high shear measurements were done. Additionally, to show the fast regeneration of the product after it has been sheared, recovery testing was done. A further issue related to product quality was the occurrence of sedimentation, which was assessed by the amplitude, - and frequency sweep tests and checked by particle size distribution measurements.

1.2 Description of the product

As mentioned earlier, Rhinocort® contains budesonide as the active pharmaceutical ingredient, which belongs to a group of so-called corticosteroids, that are targeting the inflammation occurring during allergic reactions. Budesonide is widely used and has not yet been reported for toxicity, although precautions should be taken when using the medication, as it may lead to nasal mucosa irritation, sleeping disorders, anxiety, etc. [1].

The product itself is an off-white suspension, containing several other excipients besides the budesonide to improve its quality and bioavailability. Rhinocort® is available in two different dosage forms, namely the 32 µg/dose and the 64 µg/dose [1], [2], from which the latter formulation is presented in figure 1.



Figure 1. The product of McNeil is presented, 64 µg/dose Rhinocort® Aqua [picture taken on-site].

For using the medicine, first, the patients should blow out their noses and shake the bottles in order to obtain uniformity. Then the protective cap should be removed, and the spray pump should be inserted into the nose. After pumping out the required amount of drug, the pump should be removed from the nostril and the protective cap should be placed back onto the device. The procedure should only be repeated as prescribed by healthcare professionals [1].

2. Background

2.1 Biological background - allergy

Allergic rhinitis is caused by a harmless substance, an allergen, which is seen as an invading substance by the immune system. Overall, there are more than 400 million people suffering from its effects and this number is constantly increasing due to various factors, which include pollution and exposure to smoking. It has also been shown that genetic factors play an important role in its development. Being affected by allergic rhinitis has many drawbacks in one's life, as it has an impact on the efficacy of work or studying [3]. Another negative aspect of suffering from rhinitis can be seen as a heavy burden on society, as it has been shown that the average number of working days missed results in an estimated net loss of € 2.7 billion per year in Sweden [4]. Identifying rhinitis is often overlooked, although it has been shown that there is a direct connection between having allergic rhinitis and the severity of asthma [5]. To determine the presence of allergic rhinitis, there are two methods. These tests are the skin-prick test, which involves bringing the allergen into direct contact with the skin and observation of IgE levels. Out of these tests, the skin-prick test is preferred because of its time efficacy [5].

2.1.1 Process of allergic sensitization

The process by which the allergy symptoms occur is caused by the dendritic cells presenting the allergen to the T cells, which in turn trigger the Th2 cells to release different mediators, such as the IL-4. This interleukin aids the class-switch from IgG to IgE in the antibody-producing B cells. Specific IgE receptors can be found on the mast cells, thus the IgE can bind to these and induces the release of histamine, which results in the problems associated with allergic reactions [3]. This process can be seen in the representative figure below (figure 2.).

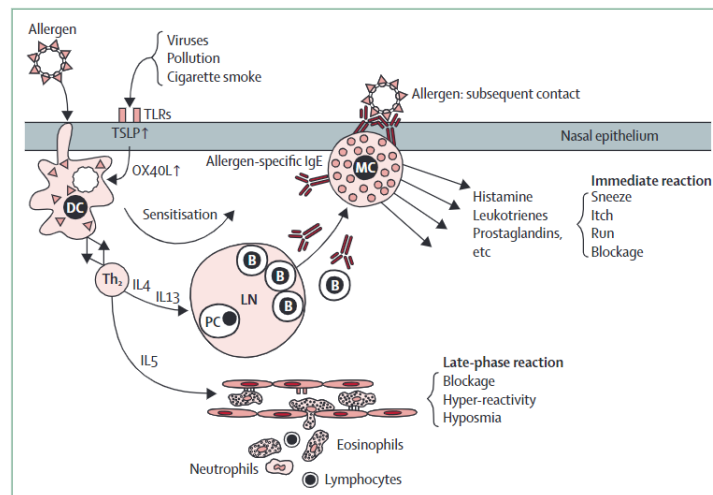


Figure 2. Showing the sensitization process from DCs taking up the allergen to the symptom development by mast cell degranulation [3].

The function of Th2 cells is not only to induce the class-switch but also to release different mediators that result in inflammation, thus making the membrane layer in the nasal cavity more responsive [6].

2.1.2 Treatment

For the treatment to be effective, taking preventative measures is key. By raising awareness of the different influencing factors in childhood, the patients could avoid being exposed to these. Furthermore, the treatments available on the market help to have the allergic symptoms under control, such as nasal sprays containing corticosteroids. Another great therapy is enhancing the immune system by triggering it with frequent allergen injections; this kind of treatment is called immunotherapy [3]. Additionally, antihistamines can also be used, although one of the disadvantages occurring is the tranquilizer effects, although these have been reduced in the newer generation of these types of medicines [6].

2.1.3 Delivery to the nasal cavity

As it has been mentioned before, allergy poses a severe burden on society and the quality of life, thus treatment is needed. If the patients have difficulties swallowing, the drug delivery into the nasal cavity can be an alternative to oral administration [7]. Furthermore, as the nasal cavity is rich in capillaries and has a large interface, it can replace the parenteral route, as the extent of absorption through its epithelium is almost the same as by injection [7]. For understanding the advantages and disadvantages of this route, the anatomy of the nose must be considered; the main anatomical structures can be seen in figure 3.

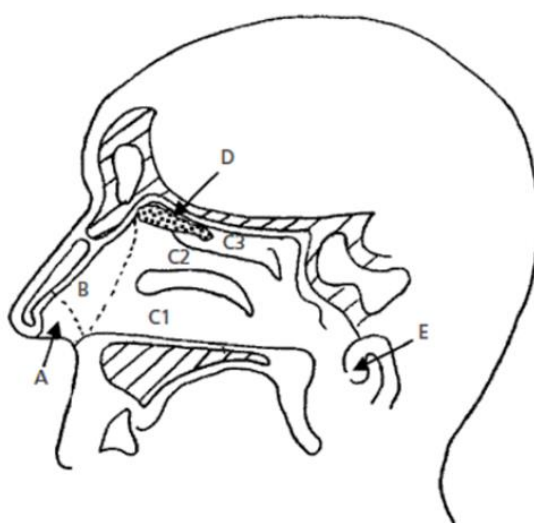


Figure 3. Representation of the main structures in the nasal cavity [7].

The nose is the first structure of the respiratory tract, and its main functions are warming up and moistening the incoming air, as well as filtration [8]. As figure 3. shows, the nose can be separated into three main structures (B, C, and D), as A represents the entry to the nasal cavity (nasal vestibule), while E shows the nasopharynx which leads to the throat. The letters B, C, and D in figure 3. show the vestibular region, which is primarily important in filtration, the turbinate region that is further divided into three different parts (C1, C2, and C3) and the olfactory region which distributes the drugs to various regions in the brain [7]. Within the turbinate region, the various types of cells present can be covered with microvilli, which are accountable for enlarging the interface, so the medicine uptake is most efficient here; or cilia, which are in constant movement, thus promoting the elimination of foreign substances [7]. This mucociliary clearance can be viewed as one of the disadvantages of nasal delivery, also this route is restricted to low molecular weight products and requires high lipophilicity, as the mucosa itself also has this characteristic [8].

Furthermore, the formulation of the medication should be carefully considered, as the success of bioavailability is highly dependent on the pH, viscosity, and the various types of excipients used. As for the delivery of the drug, there are different types of forms available on the market, these being nasal drops, sprays, gels, powders, etc. [8]. Although the usage of the drops is easy, they often require the patients to bend over for delivery, thus making it less attractive. Other available strategies are, the delivery by catheter, which is only possible with special assistance, and by using pressurized meter-dose inhalers (pMDIs), although these have been relegated to the background as the propellants used for their production turned out to cause irritations. As an alternative to all these methods, nasal sprays have received a lot of attention, as they are convenient to use, and the drug dose is replicated at every administration [9]. The nasal sprays usually deliver suspensions into the nasal cavity, which exhibit different rheological behaviours [10] and contain various excipients [8].

2.2 Suspensions

As the product of interest is a nasal spray suspension, it is of high importance to gain understanding of the properties of a suspension. These belong to a group of so-called dispersed systems, containing the liquid solution in which the insoluble API is dispersed. They are widely used for drug administration into humans and animals, and for protection against various pests. But as all other kinds of formulations, they have to be monitored to meet specifications, guarantee uniformity of dosage, have an acceptable sedimentation process and viscosity [11].

Unfortunately, in dispersed systems, the settling of the particles is inevitable in a long period, but there are factors that can be influenced, such as the size of the particles and the viscosity of the liquid phase. This settling in the system is caused by gravity which is dragging the particles down and leads to sediment formation, thus can pose a threat to the quality of the product. For counteraction, the Brownian motion keeps the particles in constant movement, but as the particle size is growing it is harder to overcome gravity. To prevent this from happening, additives can be added to the liquid phase, which enhances the stability of the suspension by creating a highly structured gel network [12].

As mentioned before particle size plays an important role in the sedimentation process, and it is an easily changeable factor, thus during the formulation work, it must be considered. Although the fact that the smaller the particles are, the likeliness of the sedimentation decreases, does not mean that the particle size should be as small as possible, or the drug may

not be as effective. Also, the viscosity of the liquid phase can affect the sedimentation, as the larger this variable is, the slower the sedimentation build-up will be [12].

For the analysis of the particle size, there are different techniques, such as sieving, microscopy, laser scattering, etc., all having their advantages and disadvantages. Although microscopy can identify individual particles, the analysis with this equipment is considered to take too long and ineffective with smaller particles than 3 μm . Another relatively affordable method is the sieving technique where sieves with progressively decreasing hole diameters are placed one under the other, but due to cleaning issues and it only being effective in the case of powders, it is not relevant from my perspective [13].

The method that is mostly used for particle size distribution in suspensions is laser diffraction, in which the light (laser) travels through the target sample and based on the scattering, the particles can be characterized with the help of an analyzing computer [13]. The data received after the computerized evaluation can be best understood in a way that the bigger particles scatter in lower angles, and they give stronger signals [14]. This is further described in the methodology part of my thesis, in section 4.2.

3. Rheology and fluid behaviour

Rheology studies the flow behaviour of different fluids and their distortion to the given pressure. Viscosity is an important aspect of the flow, as it can be described as the resistivity against flow and can be understood when looking at a two-plate model (see figure 4.). This model describes fluids as having different layers with various velocities, and by the application of force, the upper layer moves away, while the bottom one is fixed [15].

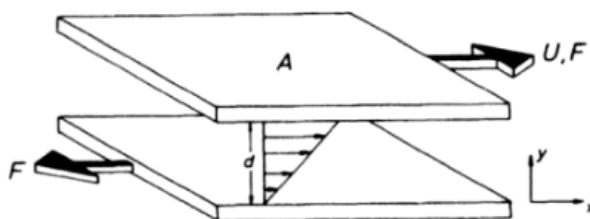


Figure 4. Two-plate model representing the shear stress and shear rate [10].

In figure 4., the shear stress and shear rate can be identified, and dividing these two gives the viscosity. Shear stress can be presented by dividing the applied force (F) with the area affected (A), while the velocity (U) of the upper plate divided by the distance (d) between the plates gives the shear rate [16].

3.1 Newtonian behaviour

There are two subgroups of fluids based on the connection between shear stress and shear rate; the fluids that have a linear relation between these two, are called Newtonian fluids and their viscosity does not alter with the change of these variables [15]. The equation that is used to calculate the viscosity (η) of Newtonian fluids, is the following:

$$\eta \text{ (Pa} \cdot \text{s)} = \frac{\text{shear stress}}{\text{shear rate}} = \frac{F/A}{U/d} \quad (1)$$

There are several methods for quantifying the viscosity of various Newtonian fluids, such as the capillary viscometer, the pressure-driven methods, the rolling ball measurement, the rotational viscometers, etc. Some of these methods have been described in the European Pharmacopoeia and are well-known and used [17].

One of the most used is the capillary viscometer, shown in figure 5., and it is based on the measured time that the fluid needs to travel through a known-length tube. Based on the known constant of the viscometer the kinematic viscosity can be calculated [17].

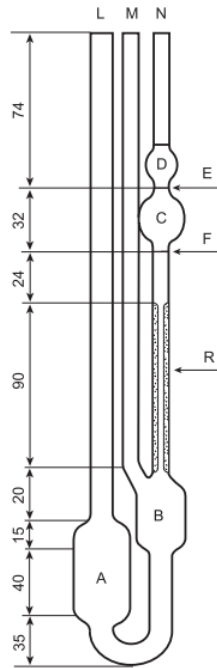


Figure 5. Representation of the capillary viscometer for measuring non-Newtonian fluid viscosity [17].

The theory behind the rotational instruments is that they contain rotating elements that are shearing the given fluids [18]. In the case of viscometers, the force needed to move the submerged piece in the liquid is measured, thus knowledge can be gained regarding the viscosity. On the other hand, with the rotational rheometers, the fluid of interest can be subjected to different shear rates. For this type of instrument, there are different types of geometries accessible, such as the coaxial cylinders, cone and plate, and parallel plate which can be seen in figure 6. [19], these types of equipment are also capable of measuring non-Newtonian viscosity [11].

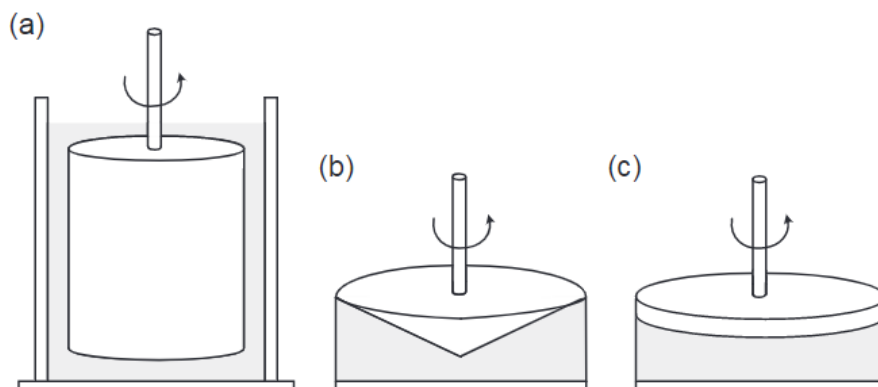


Figure 6. Different geometries that are available for a rotational rheometer [19].

The different types of geometries presented in figure 6. are as follows: the first one (a) represents the coaxial cylinder, where the liquid is trapped between two interfaces; this case is

used for suspensions. The second picture (b) displays the cone and plate method, in which case the accuracy of the measurements is highly dependent on the angle between the two parts. On the contrary, in the case of the third picture (c) the angle between the two surfaces is zero, thus making this parallel plate geometry simpler [19].

3.2 Non-Newtonian behaviour

In contrast to Newtonian fluids, the viscosity of non-Newtonian fluids is dependent on the change of shear rate and shear stress [15], and cannot be described with the equation seen above (equation 1.).

3.2.1 Shear-thinning and shear-thickening behaviour

The different types of non-Newtonian fluids have been put into subgroups based on how they act to the applied stress. In the case of **shear-thinning** behaviour the fluid demonstrates a viscosity decrease to the applied force, while on the contrary, the growth of the flowability can be examined in **shear-thickening** fluids due to increased shear rate. These behaviours are also referred to as pseudoplasticity and dilatancy, respectively [10]. The below-seen figure 7. represents these behaviours.

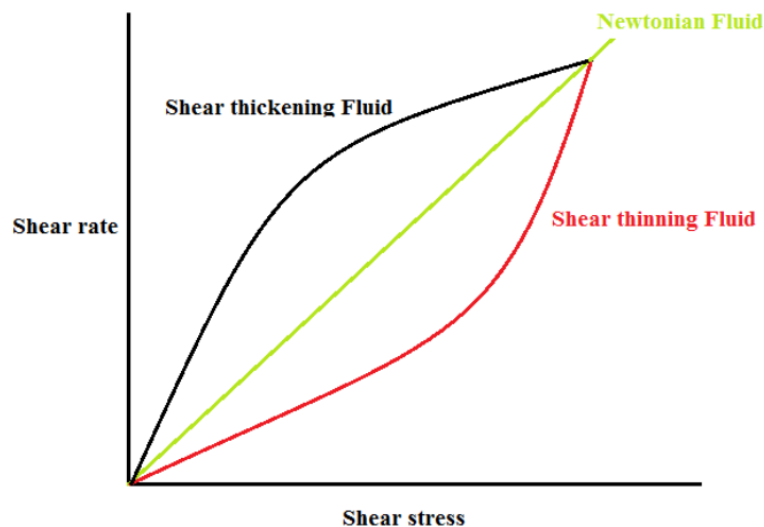


Figure 7. Showing the shear-thinning and shear-thickening behaviour in comparison to a Newtonian fluid [20].

Some common examples of these kinds of behaviour can be found in everyday products, such as shampoo or corn-starch-water mixture. The latter belongs to the shear-thickening fluids, as by harsh mixing of the material, it behaves solid-like. On the other hand, the viscosity of the shampoo decreases as it is squeezed out of the bottle, thus exhibiting shear-thinning characteristics [21].

3.2.2 Thixotropic and rheopectic behaviour

There are two types of non-Newtonian fluids, in which the viscosity is dependent on the duration of being exposed to shearing. These time-dependent characteristics are called **thixotropy** and **rheopexy** [22], in the latter case, the substance subjected to higher shear has increased viscosity [10].

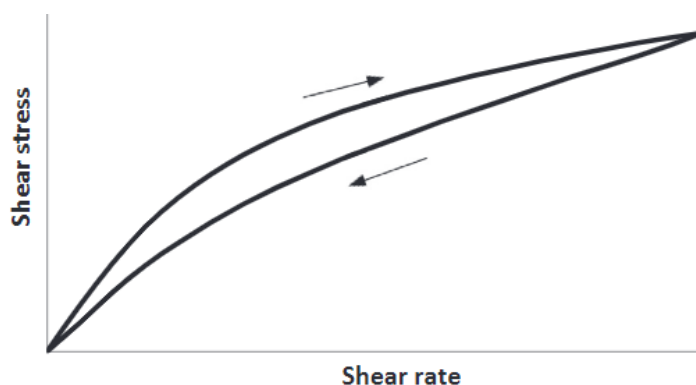


Figure 8. Representation of thixotropic behaviour and formation of hysteresis loop [19].

The nasal spray product of interest has thixotropic characteristics [23], and this behaviour can be seen in figure 8. This property is best described as the breakdown of the structure due to applied force, but when this stress is terminated, the material slowly returns to its original structural state [24]. This slow regeneration can be examined in figure 8. above, as the up, - and down curves are misplaced from one other.

The term thixotropy itself used for identifying these kinds of behaviours was introduced in the early 1900s and originates from a combination of Greek words [24]. The changes in the microstructure are due to damage caused by the applied force and the counteracting Brownian motion, which triggers the different particles to couple with one other [24].

3.2.3 Excipients with thixotropic behaviour

The excipients responsible for achieving increased viscosity in Rhinocort® (giving the thixotropic characteristics) are microcrystalline cellulose (MCC) and sodium carboxyl methylcellulose (NaCMC), a combination of which is widely used in the industry and is known as Avicel RC-591 [25]. The structure of cellulose can be seen in figure 9. below, representing the different regions found within the material, which are the crystalline, - and amorphous parts. It is built up from glucose units by C1-C4 connections and can be subjected to acidic treatment in order to alter the structure [26].

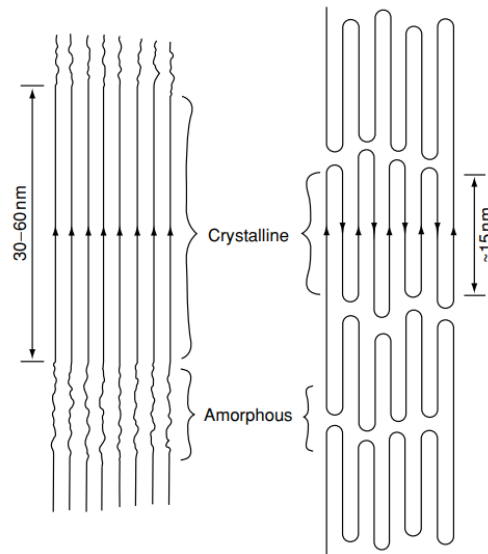


Figure 9. Different regions found in natural cellulose [26].

It has a great benefit in comparison to the different polymers, as it is biodegradable. MCC is derived from cellulose and obtained after acidic hydrolysis [27], during which it turns into a more resilient structure [26]. The NaCMC is produced by etherification of the OH groups present in the cellulose [28] and is used as a thickening agent [26], thus this is the part truly responsible for enhanced viscosity in the product [11]. A review article made by *Trache and co-workers* pointed out the diversity of the MCC use, and the different features of this material, as it is well known for being inert, non-poisonous, and helpful in adjusting viscosity [27].

Dolz-Planas et al. have conducted some experiments to study the thixotropic behaviour of different concentrations of MCC:NaCMC and the results showed that the connection between the growth in viscosity was not proportionate to the increase in concentration [29]. Additionally, it has been shown that an additional polymer can also contribute to the improvement of viscosity [30].

Throughout some tests carried out, a decrease in viscosity could be examined at higher storage temperatures, which presumably occurred due to the destruction of the polymer chain [31]. This phenomenon was already stated by *Dolz-Planas et al.* based on the experiments conducted, which showed the temperature dependency of the thixotropic behaviour. Additionally, the data retrieved showed a connection between the time of the disturbance of the liquid (agitation time) and the degradation of the structure, as the area between the up and down curves increased with higher agitation time [32].

3.2.4 Other excipients in the nasal suspension

As mentioned in section 2.2, in pharmaceutical suspensions small, firm particles are present in a different phase. Also, these suspensions consist of various excipients to aid the formulation; besides the ones listed above (MCC and NaCMC), which not only enhance the viscosity but also serve as suspending agents. The presence of an osmotic agent, buffer, preservative, and surfactant is also a necessity for successful drug delivery [33].

Anhydrous dextrose is contributing to the formulation as an osmotic agent, meaning that it creates an osmotic pressure as such that can be found within the body [22]. In order to maintain the stability of a product preservatives are needed, which inhibit the growth of various microorganisms [33]; the preservative used in Rhinocort® is the **potassium sorbate**. To set the pH of a suspension **HCl** is used [11], and as a chelating agent, **EDTA** is used for filtering out metal ions [34]. In a suspension, a surfactant must be used in order to make sure that the tension between the medium and the medical particles is lowered, such surfactant is the **polysorbate 80** [33].

4. Methodology

4.1 Rheometer and RheoCompass

As mentioned before, there are several methods for measuring viscosity, but considering the thixotropic (non-Newtonian) characteristics of the material and the equipment available at the company, my focus was on the rotational rheometer with double-gap geometry (according to the test method). It measures the resistance force exerted by the fluid on the sunken body and can thus determine its viscosity. The equipment used is an Anton Paar MCR 302 rheometer (seen in figure 10.) connected to the evaluating software, RheoCompass.

The analyzing methods and experimental setups used throughout the thesis are further explained in the following sections (sections 4.1.1 – 4.1.4.).



Figure 10. Anton Paar MCR 302 with double-gap geometry in use [picture taken on-site].

4.1.1 Three-interval loop test

The material has thixotropic characteristics, as stated previously and one of the most common methods for determination of this behavior is the three-interval loop test, in which the material is sheared to a different extent. The first shear rate applied is low, the second interval demonstrates the forces that the material can be subjected to due to everyday use, thus it is a high shear rate. Throughout the third interval, the shear rate is low again to represent the structural regrowth. These kinds of measurements when the shear rate is set, are called

controlled shear rate (CSR) studies. Based on this three-interval method presented above, by using the RheoCompass software, we can obtain different data, which gives a better understanding regarding the percentage of restoration for a defined period of time [35]. In the case of calculating the recovery ratio, the software gives the percentage of the viscosity difference between two values after a given time; these points are usually the starting time and any chosen time. Based on this information the time by which the product fully recovers, can be predicted [35].

The plan was to use this method to represent the period that our thixotropic material, the Rhinocort® requires for regeneration after it has been sheared.

4.1.2 Hysteresis loop

To best examine the time-dependent characteristic of Rhinocort®, hysteresis loop tests were used. The sample was sheared from low to maximum shear and then the shear rate returned to the initial rate. The viscosity was evaluated at the highest shear point. The outcome of the measurements were two different diagrams, one of which is called the flow curve and shows the relation between shear rate and shear stress. The second curve generated is the viscosity curve displaying the viscosity in relation to the shear rate. At maximum shear, the viscosity was calculated and was shown in the report.

Based on the hysteresis loop, knowledge can be gained on the features of the substance, meaning that we can differentiate between shear-thinning and shear-thickening fluids based on the placement of the various curves. Just by looking at them, we can determine if the material has shear-thinning characteristics as in this case the ramp going up is placed higher than the down curve; the opposite is true in the case of shear-thickening fluids, as here the curves switch places [35].

This measurement is in everyday use at the company (according to the test method) to determine the viscosity of the product at a given shear. This loop measurement can also be used to determine structural reparation, as measuring the viscosity once and letting the material rest in the machine, then running the same loop gives valuable information on how long the material needs to retain its initial state.

Flow and viscosity curve

To gain a better understanding of the rheological behavior of a material, the most used diagrams are the flow and the viscosity curves. In the flow curve, the relation between the shear rate and

shear stress is presented which is linear in the case of Newtonian fluids, but in most pharmaceutical suspensions this relationship is non-linear.

On the viscosity curve, the viscosity is presented as a function of shear rate, so from this data we can determine if the material is shear thinning or shear thickening, meaning that by the applied shear the viscosity either increases or decreases [35], [36].

4.1.3 Amplitude sweep

By using the MCR 302, an amplitude test can be carried out which uses growing vibration amplitude, while the frequency is kept at a constant low level. This test gives insight into the characteristics of the material by showing the storage (G') and the loss (G'') moduli and displaying the linear viscoelastic region, known as LVER, which shows at what point the structure begins to break down, also a longer region represents a well-dispersed material [37]. The region is linear when the strain is not significant enough to cause structural deformation, but once it is exceeded, different behaviors can be read from the graph based on the G' and G'' curves [35], [36].

If the G' curve is positioned higher, then the material of interest exhibits viscoelastic solid behavior; in comparison to this, if the loss/viscous curve is higher, the material has viscoelastic fluid behavior. This amplitude sweep method is also often used in various types of gels to see the sol-gel transition point, as it is the point where the two curves cross and G'' exceeds the resting modulus. Furthermore, this test is used as a basis for the frequency sweep method, since it gives the initial strain when the material is in the non-linear range [35], [36].

4.1.4 Frequency sweep

As mentioned before, the starting point for this measurement is based on the data retrieved from the LVER that was given after the amplitude sweep test. After overcoming the linear region, the frequency in this test is continuously changed to see how the material reacts to it. This measurement plays an important role in characterizing paints, as it gives great information about their behavior and microstructure. For these kinds of measurements, the G' , G'' , and the complex viscosity are usually represented on the same graph for easier interpretations. By looking at the data obtained, we can determine the likelihood of sedimentation appearance, as a material whose viscosity is not dependent on the different frequencies is not likely to have deposition formation, while in other materials where the viscosity becomes dependent on the frequency, sedimentation might happen [37]. A graph obtained from a frequency sweep test can be seen below in figure 11, presenting the G' , G'' and the complex viscosity (η).

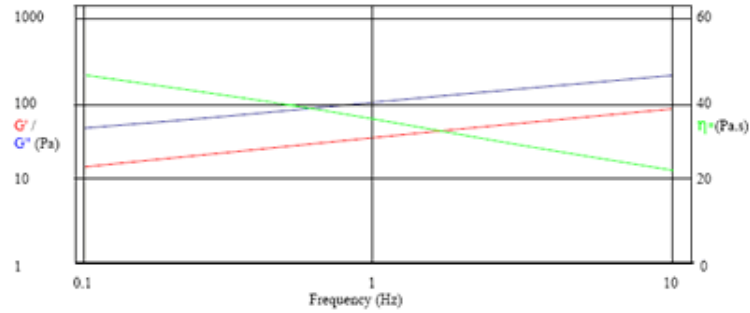


Figure 11. Showing a frequency dependent system that is likely to sediment [37].

4.2 Particle size distribution

The apparatus used for determining the particle size distribution is presented in figure 12. below, and is called Malvern Spraytec. The laser passes through the sprayed sample and by using the Mie theory of light scattering the particles are analysed [38]. The reason behind the popularity of the laser diffraction method is that it gives a wide range of coverage over various particle sizes, due to its easy way of handling and speed [39].



Figure 12. Presentation of the laser diffraction system with the different parts [13].

The measurements were done according to an old test method obtained after the product transfer from AstraZeneca. Based on this method, three different bottles were measured every day, and three sprays were inspected in each individual bottle. From these, the average value was received and plotted in a Minitab graph, which can be seen below under the result section in graph 12.

The aim of these kinds of measurements was to inspect the size of budesonide, as all other excipients are considered to be dissolved in the liquid phase. The idea was, that the knowledge about the size of budesonide particles might give an explanation about the settling problem, as bigger particles have a higher tendency to form sediments. Also, this test has not been run for

two years now, as it was only required for the US market, thus getting these results gave a great update about the quality of the product, as the size and volume percentage of particles should be within the specification limits. The importance of monitoring this lies in the fact, that smaller particles are posing a severe health risk as they are traveling to the lungs, while the bigger particles also do not reach the desired effect as they are usually swallowed [40].

The data that can be retrieved from the laser diffraction analysis is the D_{10} , D_{50} , and D_{90} values, as well as the span. These D values serve statistical reasons as they stand for different points on the distribution curve. As can be seen from figure 13., these points respectively mark the position on the graph, below which 10%, 50% and, 90% of the particles are present. With the help of these values, the small particles can be filtered out by using the D_{10} value, while the big particles are also represented with the aid of D_{90} [14].

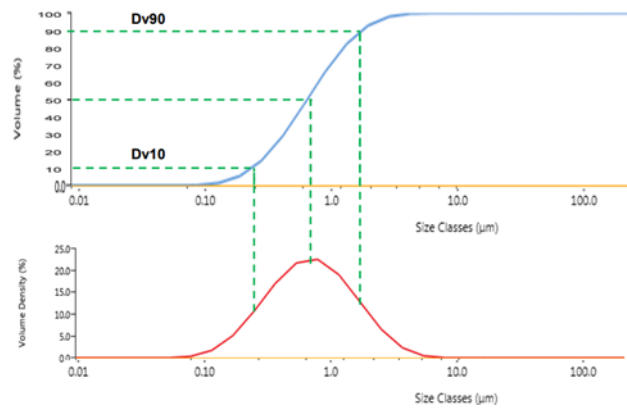


Figure 13. Showing the various D values and their meanings [14].

The span is a calculated value, received from the D values mentioned above, which shows the divergence from the D_{50} . The equation to calculate this can be seen below (equation 2.):

$$Span = \frac{D_{90} - D_{10}}{D_{50}} \quad (2)$$

4.3 Placebo formulation

Placebos were formulated in order to achieve higher initial viscosity values. As the recipe is confidential, only the steps of the formulation are described here, not the amounts of the different excipients. The Avicel used for these experiments was mixed together by me using 22 w/w%, 15 w/w% or 13 w/w% sodium carboxy-methylcellulose and the right amount of microcrystalline cellulose.

After measuring the needed amount (measured on an analytical scale) of pre-mixed Avicel into a flask, water was added, and the mixture was stirred on a magnetic stirrer at room temperature for 5 minutes, or until it was deemed homogenous. In a separate flask, the anhydrous dextrose and potassium sorbate was measured and mixed with water for 1 minute, then added to the Avicel mixture. EDTA was also pre-dissolved in water in a separate flask, then added to the Avicel mixture. Polysorbate 80 was pipetted into the flask containing the other excipients by using a plastic pipette.

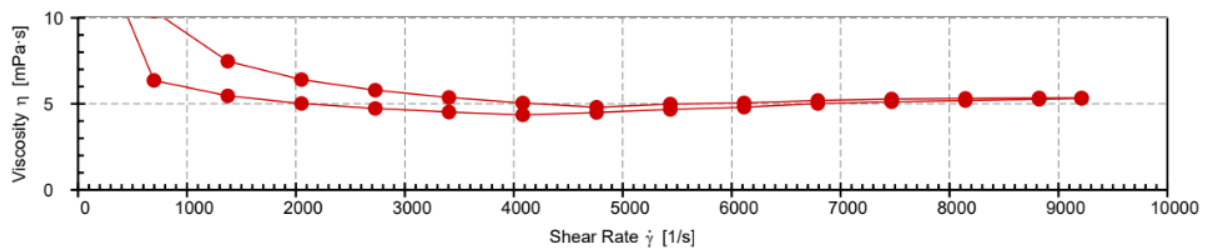
The mixture containing all excipients was stirred for 1 hour at room temperature, after which the pH of the mixture was set by using HCl and indicator paper.

After the placebos were produced, they were tested in the rheometer to see if viscosity change was achieved.

5. Results

Before setting up the experiments presented below, it is important to mention the path that led to them, namely the **method development** by using old AstraZeneca samples.

Firstly, the **high shear method** was developed to see the resistance of the material and to understand why the test method states that measurements are made at a certain shear rate. This method was successfully developed and used later, the graph displaying this first measurement can be seen below in graph 1. According to the test method the three-interval measurements are running from $20 \frac{1}{s}$ up to $1740 \pm 30 \frac{1}{s}$ and then back again to the initial ($20 \frac{1}{s}$) state.



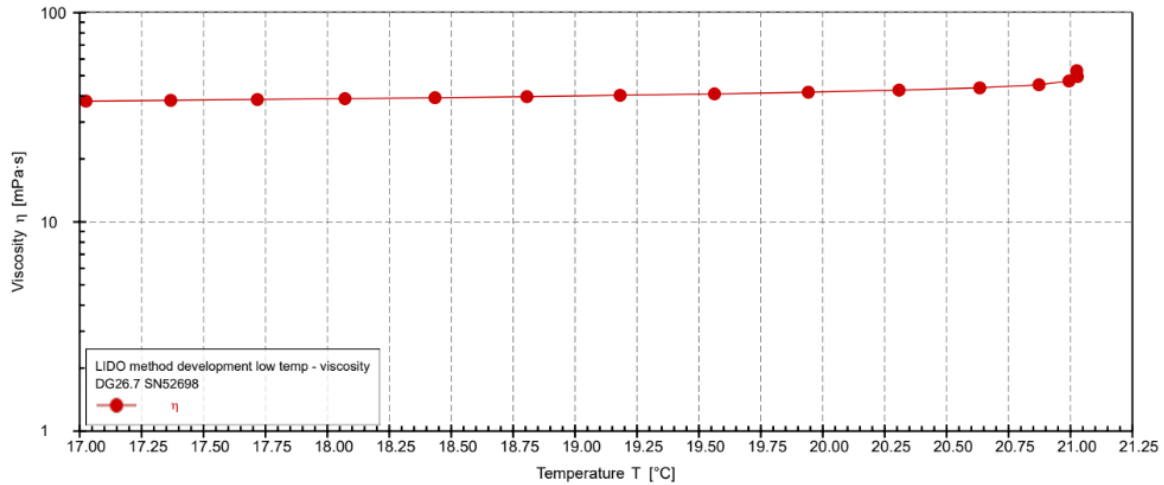
Graph 1. Representing the method development for the high shear method.

It can be seen above in graph 1. that the original idea was to measure up to $10000 \frac{1}{s}$ shear rate, but this could not be reached by the equipment, thus in all the other high shear measurements the graph is only made up until $9500 \frac{1}{s}$. Also, this experiment explained the reason why the test method states that the measurements should be done at $1740 \frac{1}{s}$, since it is located at the beginning of the linear (equilibrium) state.

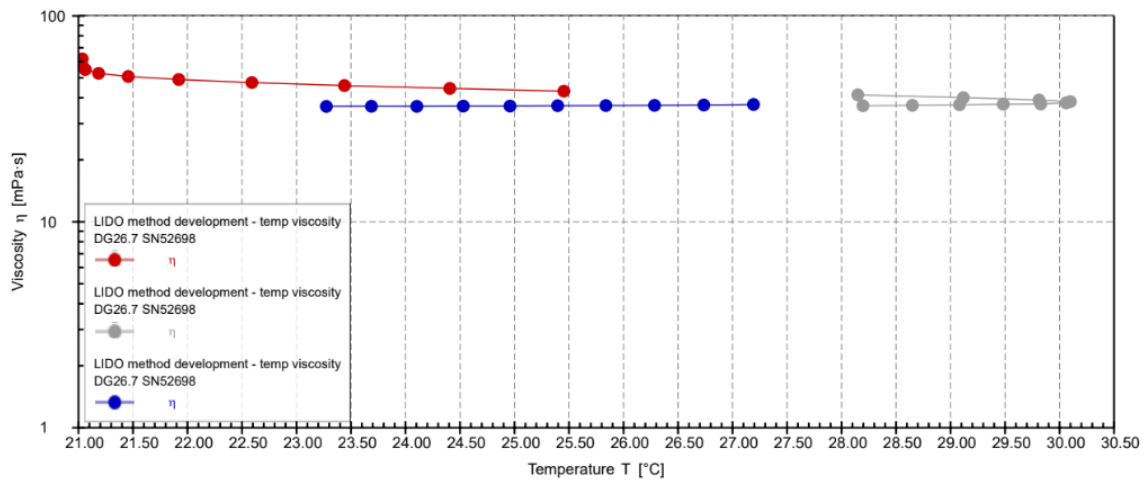
To test whether there is potential in investigating the **temperature-dependent viscosity**, a method was set up to measure the viscosity change as the function of temperature, while holding constant shear stress. The idea was to decrease the temperature until the lowest stability limit is reached, which is $2 \text{ }^\circ\text{C}$. However, the equipment was too slow in cooling and could only reach $17 \text{ }^\circ\text{C}$ when starting from the specified temperature for the test method ($21 \text{ }^\circ\text{C}$), this graph is shown below (graph 2.). When warmed, the same phenomenon was examined, as the viscosity seemed to decrease with increased temperatures as well, starting from room temperature and reaching up to $30 \text{ }^\circ\text{C}$. The graph displaying these results can be found below (graph 3.).

This process also took a long time, thus leading to the realization that all measurements should be done at $21 \text{ }^\circ\text{C}$. Despite this graph showing that the best possible values can only be obtained

at room temperature, heating, and cooling of samples was done. Also, it was successfully executed and disproved this initial measurement, as the viscosity increased with higher temperatures (these experiments are explained below in section 5.1).

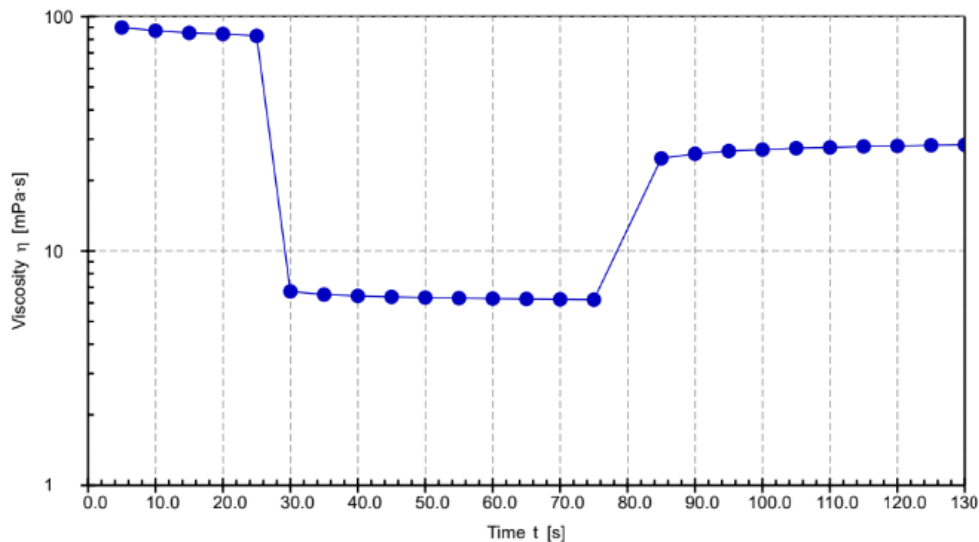


Graph 2. Representation of the temperature dependence of the viscosity and inspection of a decrease in viscosity values by decreasing the temperature.



Graph 3. Representation of high temperature dependence of the viscosity, showing a decrease or no change in the value.

The description of the RheoCompass software stated (mentioned in section 4.1.1) that it is possible to get information on the **recovery ratio** of the product based on the difference between the initial viscosity value and the viscosity after a chosen time. Although the method setup seemed to work as it displayed the three-interval test and presented the viscosity as the function of time (seen in graph 4.), it did not display the recovery percentage as promised.



Graph 4. Showing the three-interval test, starting from low shear, the second interval is the high shear, and the third interval is low shear again. The recovery percentage was not displayed.

After several attempts to get the percentage of the recovery in the given time, my attention shifted towards measuring the recovery in a different way as can be seen in section 5.3, which meant using the standard method as stated in the test method and seeing if an hour is enough for the structural regeneration.

Some other measurements were also made additionally to the above-mentioned tests to **ensure good quality** of the product. These tests included the ‘production’ of the lowest possible viscosity value by **vigorously shaking** and spraying the nasal suspension to see if it is still within specification or not. This experiment was done after receiving the sample on day 0. The measured viscosity value was 5.52 mPas (the undisturbed sample produced 5.98 mPas) meaning that in case of harsh handling of the product from the patients’ side, the product is still within the specification requirements (5.0 – 8.5 mPas) on day 0.

Furthermore, to allay concerns about the effect of sediment on the viscosity of the product, a test was carried out to see if it matters or not that the 4 ml of **sample** for the measurements are **taken from the sedimented** (bottom part of the bottle) or if it is taken from the liquid phase. The results showed no deviation at all, as both values were 6.41 mPas, meaning that turning the samples up and down 15 times before measuring (according to the test method) to make it uniform, might not be necessary and the sediment does not affect the overall value of the viscosity. This means that the concentration of particles in the sediment is low, thus it does not disturb the rheology created by the polymer (Avicel). Although the sediment does not seem to affect the viscosity value measured, the test method was still followed and the turning of the bottles was done in all cases to obtain uniformity.

Additionally, a test was done to show that for the **temperature dependency** tests, it does not matter if the samples are measured right after being removed from the heating chamber or if they are let to cool back to room temperature. The bottle whose viscosity was measured immediately after removal from the heating cabinet had a viscosity of 6.29 mPas, while the other bottle, which was allowed to equilibrate, had a viscosity of 6.23 mPas. This showed that waiting with the cooled or heated samples is not a necessity as they are producing almost the same results.

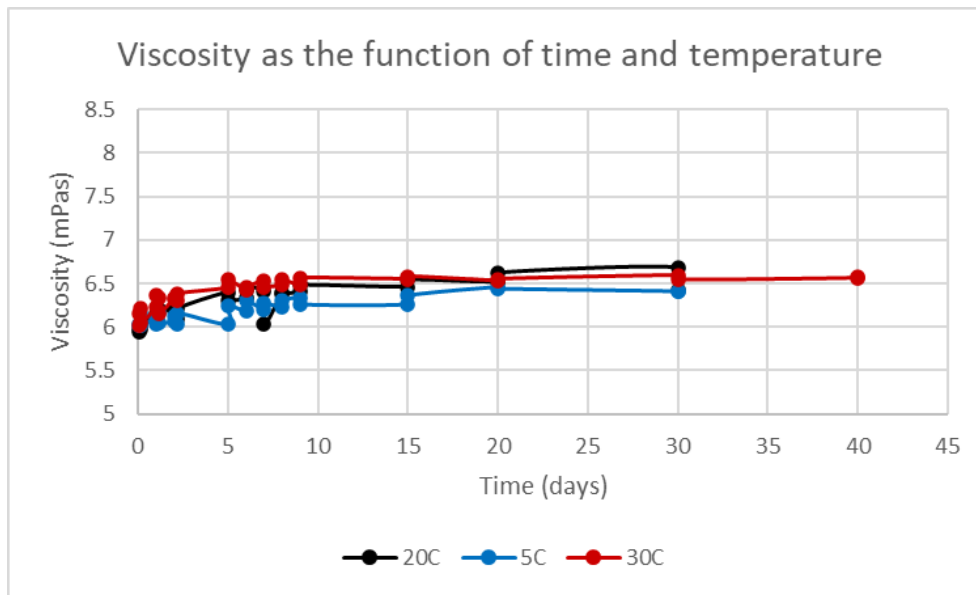
After all these preliminary method set-ups and tryouts, the real experiments have begun. A detailed description of these and their results can be seen below in sections 5.1 – 5.7. These included the investigation of temperature dependent viscosity and various shaking periods, as well as tests made to measure the recovery of the product. To ensure the quality and provide evidence that sedimentation is likely to occur in the suspension, the amplitude, - and frequency sweep tests were done. Furthermore, to provide information on the evenness of the suspension, particle size distribution was measured according to the former test method stated in the US specification. Lastly, placebos were produced with altered formulations in order to provide a higher starting viscosity value.

5.1 Investigation of temperature dependent viscosity

As it has been mentioned before the surrounding environment (the temperature) plays an important role in influencing the product's resistance to flow, thus the viscosity changes of Rhinocort® was examined at different temperatures. These kinds of experiments were running from day 0 to day 10 (up to day 40 for batch no.1).

The samples could only be subjected to a relatively narrow temperature range, from 2 °C to 30 °C, which has been established based on stability tests [41]. The samples were kept at 30 °C (30±2 °C and 75±5 % RH) in a heating chamber connected to a control system that alerts in case of temperature deviations, while the cooled samples were kept in a fridge (5 ± 3 °C).

In the graph seen below (graph 5.), the viscosity is represented as the function of time, and the various curves show the different samples with their respective temperature. In all cases the samples measured at higher temperatures are shown in red, whilst the viscosity of the cooled samples is displayed in blue, lastly, the samples held at room temperature are shown in black. The standard sample (room temperature, 20 °C) located between the cold and warm curves, serves as a basis for comparison. At all times, duplicates were taken to obtain the best possible data.



Graph 5. Investigation of the temperature dependence of viscosity in the first batch, where the blue curve marks the cooled samples (5 °C), the red curve shows the warmed bottles (30 °C), and the black curve shows the standard samples kept at room temperature (20 °C).

Before filling the liquid into the double gap, the bottles were turned up and down 15 times to obtain uniformity, but during this turning process the creation of a foam was avoided (bottles were turned carefully). By using the standard method for the measurements, the viscosity of the samples was determined on the flow curve at the highest shear rate, at $1740 \frac{1}{s}$. Plotting this data against time gave the above-seen graph 5, this shows that the samples kept at higher storage temperature produced higher viscosity values, while cooling the samples had a negative effect on viscosity. Also, what can be examined is that the product is already within the specification limit (5.0 mPas to 8.5 mPas) on day 0.

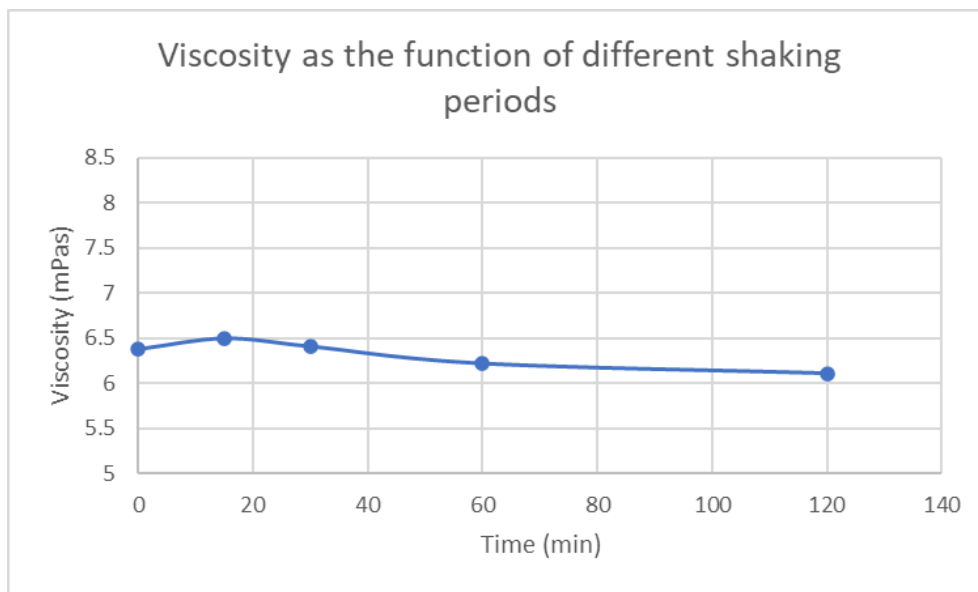
Samples were taken from the start, the middle, and from the end of production, but for the purpose of these experiments, they were randomized and put to their respective temperatures.

All the additional graphs representing the temperature dependence of viscosity in the other batches (10 batches in total were examined) can be found in the appendix.

5.2 The influence of different shaking periods

Due to gelling and sediment formation, the samples were shaken for 2 hours at the company before measuring the viscosity (although this method was not present in the test method). Given that the material is thixotropic in nature, the question arose as to how this shaking time affects (reduces) viscosity.

To provide evidence that this shaking should be left out of the viscosity measuring procedure a test was set up. For these kinds of experiments, 4 bottles were shaken for various periods, these being 15 min, 30 min, 1 h, and 2 h and the viscosity of these was measured with the standard method. For comparison reasons, a sample without shaking was also measured. By looking at graph 6. below, we can see the results of the shaking for batch no. 1, and all the other results for the following batches can be found in the appendix. As it can be seen from graph 6, the shaking influences the viscosity negatively, as it breaks down the structure, thus the product needs more time for regeneration (it is further explained in the discussion part of the thesis).



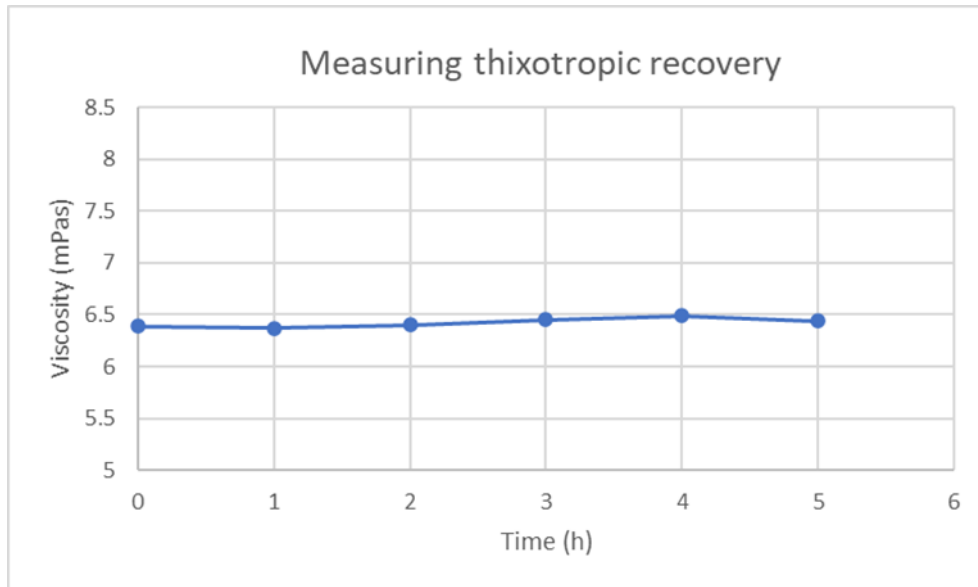
Graph 6. Representing the viscosity change due to various shaking periods.

5.3 Test for thixotropic recovery

These tests were done to give a better understanding of how fast the material returns to its original structure. Due to mixing during production and filling into the bottles, the structure breaks down, thus the viscosity decreases and as it is a thixotropic material, it needs time to regain the initial state. This measurement aimed to find a relation between the long waiting time before the viscosity measurements are taken and the destruction of the product during production.

The Rhinocort® samples were measured with the standard method using the rheometer, but after one measurement, the samples were allowed to rest in the apparatus for one hour, leaving time for it to reform. After the one-hour waiting time, the measurement was repeated, and the results were compared to see the regeneration. This kind of measurement was done on two different batches, from which the results belonging to batch no. 1 are presented below in graph 7. and the other recovery graph is shown in the appendix. These measurements were carried

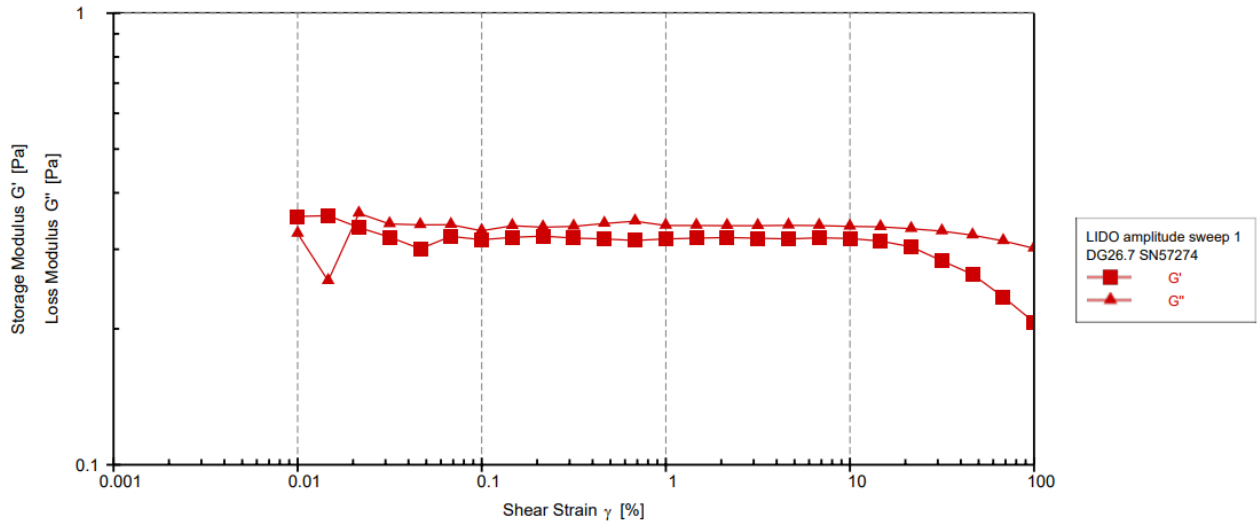
out in a 5-hour time-span, leaving one hour for structural regeneration. As seen in graph 7., the material returned to its original structure in maximum an hour.



Graph 7. Representing the time taken for full structural recovery, after the sample has been sheared.

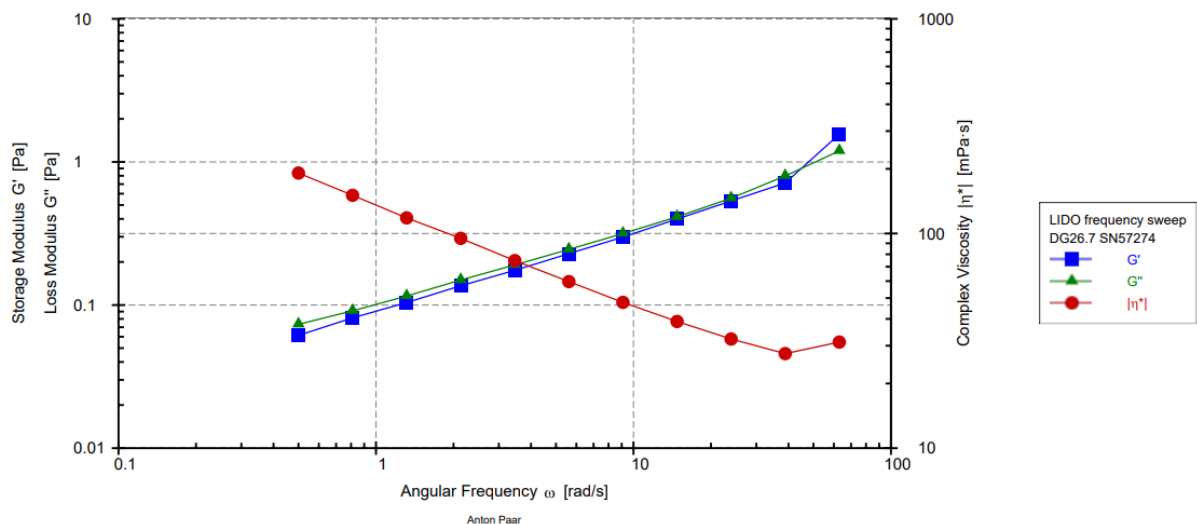
5.4 Frequency sweep and amplitude sweep

The amplitude sweep measurement was done before setting up the frequency sweep test, to determine the linear viscoelastic region (LVER), which can be seen in graph 8. below. This measurement was done based on a standard template found in the software with some modifications to fit the characteristics of the material. The angular frequency was set to $10 \frac{rad}{s}$ and was constant throughout the measurements, while the strain was increased from 0,01% to 100%. The graph retrieved from this test gave information about the point where the structure begins to break down after the LVER is exceeded as can be seen in figure 8 below. This linear viscoelastic region ends at 10 % shear strain as seen from figure 8, thus determining the start of structural disintegration.



Graph 8. Determination of the linear viscoelastic region.

As for the frequency sweep measurements, the method was set up by using a template from the software, and angular frequency was set to decrease from $63 \frac{rad}{s}$ to $0,5 \frac{rad}{s}$. On the graph below (graph 9.) the storage moduli (G'), loss moduli (G'') and complex viscosity is presented as the function of angular frequency. The G' and G'' crossover point determines the gel-sol transition, meaning that by applying a minimum amount of force to the material, its gel structure becomes fluid-like. This graph gives insight into the behavior of the material and information about the likelihood of sediment formation. Graph 9. below shows that the complex viscosity of the product is frequency dependent, thus it is likely to sediment.

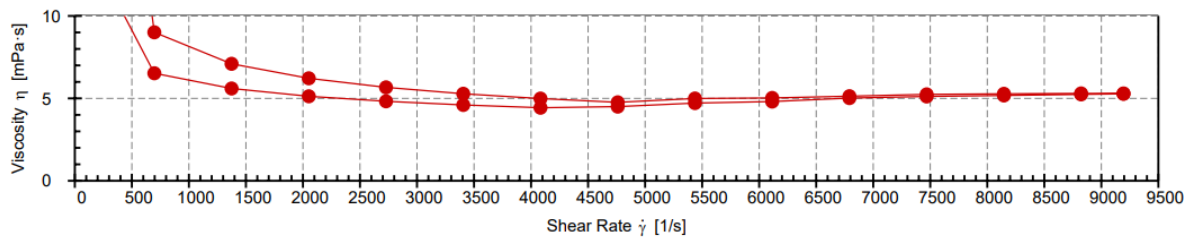


Graph 9. Showing the behavior of the product and the tendency to sediment.

5.5 High shear rate

High shear rate measurements were carried out as it has been explained earlier in the method development section. These were done to determine the resilience and sturdiness of the material

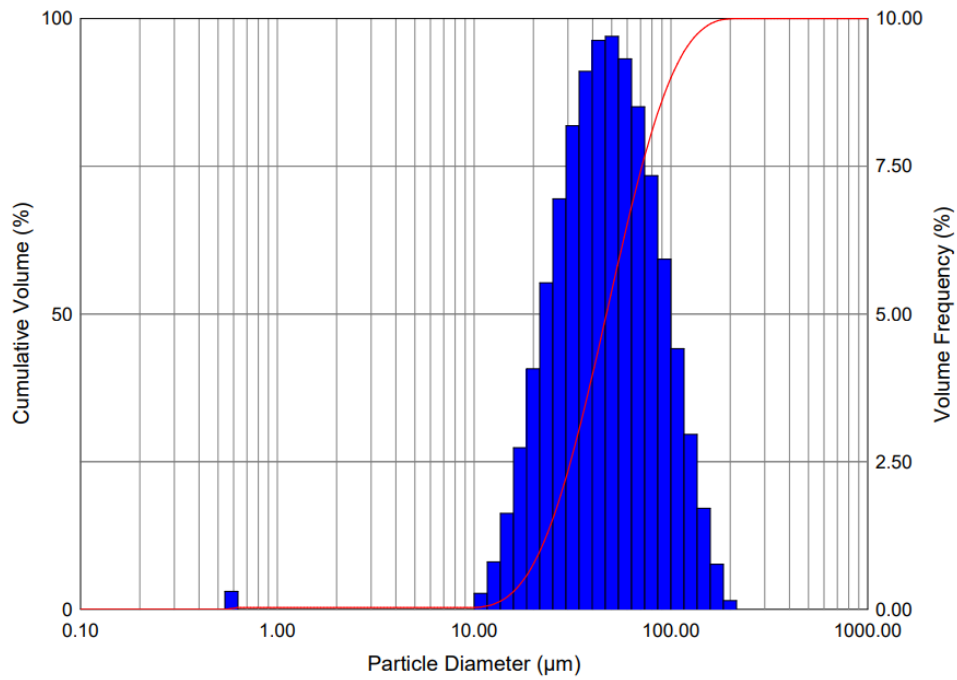
and to investigate its behavior under hard mechanical forces. The method was a three-interval measurement, starting from low shear rate ($20 \frac{1}{s}$) to the highest possible shear that the machine could tolerate, which was $9500 \frac{1}{s}$; then the shear rate started to decrease until reaching the starting point. One of these high-shear graphs generated can be observed below (graph 10), while the additional graphs from the following batches are found in the appendix. The curve positioned higher was made as the shear rate started to increase up to $9500 \frac{1}{s}$, while the curve positioned below was formed as the shear rate started to decrease back to the initial $20 \frac{1}{s}$. This hysteresis loop formation proves the shear-thinning nature of the material as explained in section 4.1.2 and shows the sturdiness of the product toward high mechanical forces.



Graph 10. Presenting the viscosity curve up to $9500 \frac{1}{s}$ to examine the robustness of the product.

5.6 Particle size distribution

The original idea to measure the particle size distribution came to mind to check for bigger particles in the sample, as bigger particles are more prone to sediment. Also, this test has not been done at the company for a few years now since it was only a requirement for the US market, thus including this in my experiments could reassure the good quality of the product. The data is given by software as seen below in a representative graph (graph 11.) and in a table (table 1.) summarizing the important values.



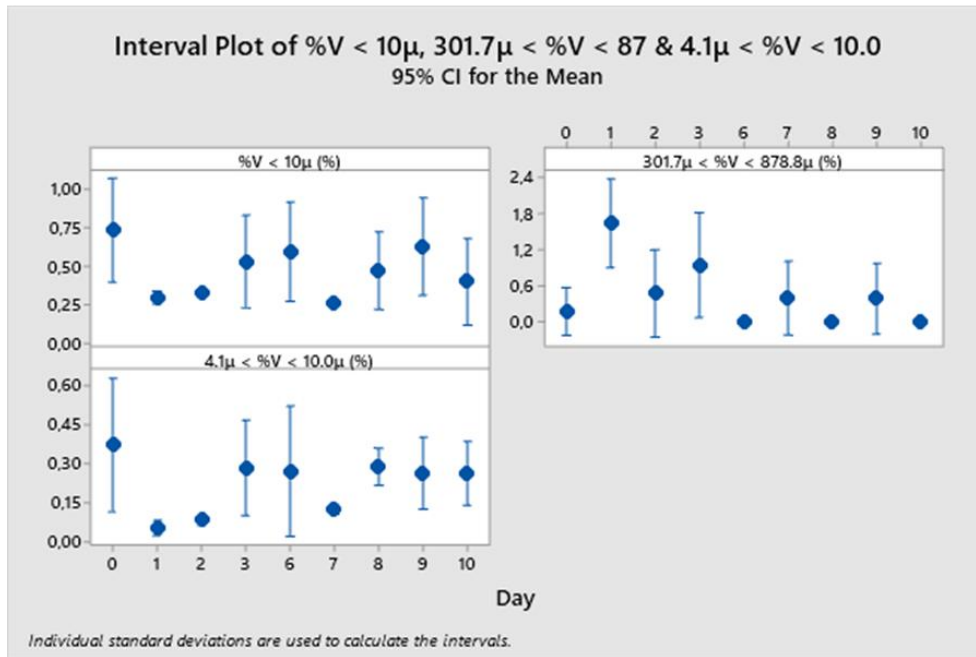
Graph 11. Showing the report made by the analyzing software. Some small particles can be examined, which are around 1 µm, the size for all other particles is between 10 – 100 µm.

Title	Average	σ	Min	Max
Trans (%)	72.0	2.022	68.4	76.2
Dv(10) (µm)	21.67	1.332	19.6	25.35
Dv(50) (µm)	46.99	5.118	40.08	61.03
Dv(90) (µm)	99.99	13.06	83.22	148.6
%V < 10µ (%)	0.305	0.1704	0.0004299	1.161
Span	1.667	0.1097	1.53	2.092
301.7µ < %V < 878.8µ (%)	0	0.8555	0	3.916
4.1µ < %V < 10.0µ (%)	0.0009842	0.1337	0.0004272	0.751

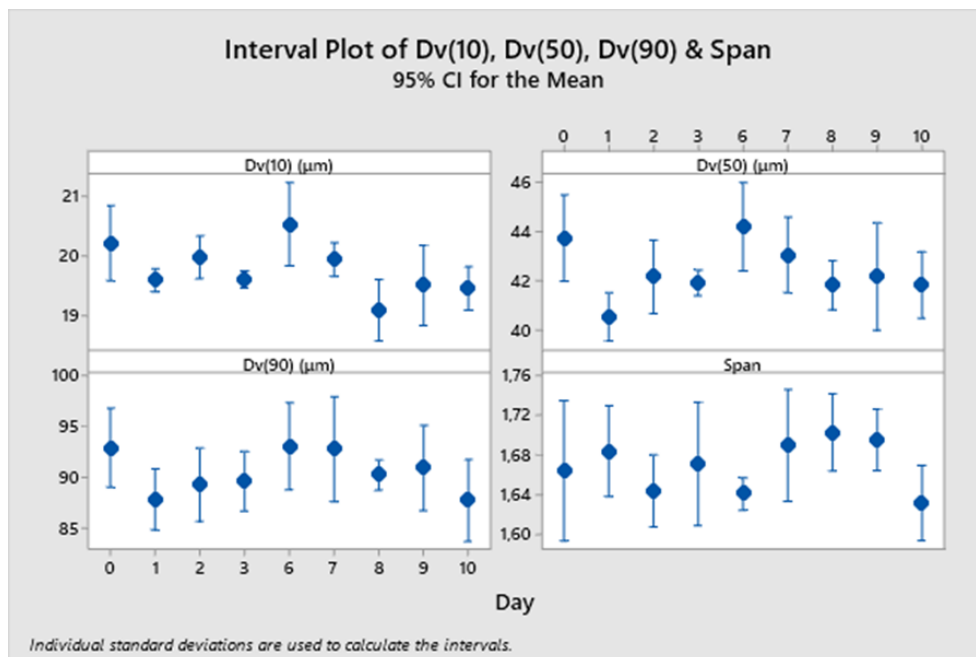
Table 1. Showing the important values from the report made by the analyzing software.

These results from all the experiments are summarized in graph 12. seen below, where the volume percentage is presented on the y-axis, while the x-axis shows the various days when the samples were measured.

In order to meet the product specification for the US market, these values have a limit within which they must stay to ensure quality. The requirements for the volume percentage of the different particles are as it follows: the volume percentage of small particles ranging from 4.2 µm to 10.5 µm should be less than 6%. For the bigger particles (between 302 µm and 880 µm) the volume percentage should not be bigger than 20% [42].



Graph 12. The volume percentage of particles of different sizes as the function of time (days).



Graph 13. The size of different particles that can be found below the specific points on the particle size distribution graph as the function of time (days). These specific points are the D_{10} , D_{50} , and D_{90} .

There are some specific values that are calculated with the software regarding the particle size distribution; these numbers are the D_{10} , D_{50} , D_{90} , and the standard deviation (span). These values are presented in graph 13. seen above, where the y-axis shows the particle size as the function of time (x-axis represents the days).

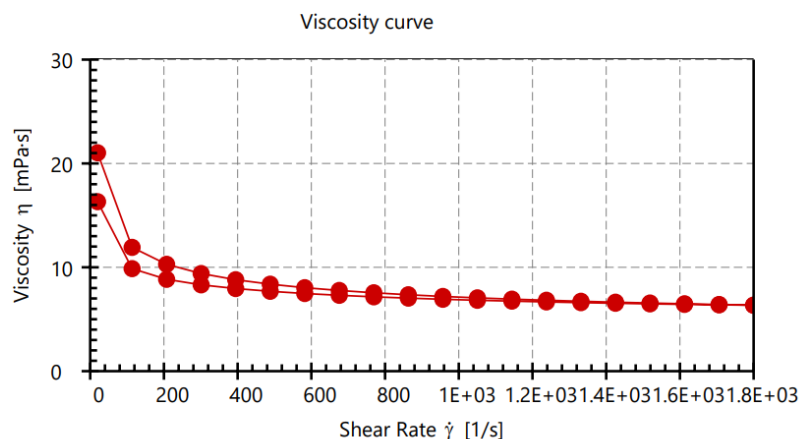
For these values, there are also some acceptance criteria that must be fulfilled. The particles below D_{10} have to be between 13 μ m and 24 μ m, this particle limit for the D_{50} is 27 μ m to 72

μm . For the D_{90} , based on the specifications the particles should be between $50\ \mu\text{m}$ to $150\ \mu\text{m}$; and lastly, for the standard deviation, the limit is 1.1 to 2.2 [42]. These specifications are all met as concluded in the discussion (section 6.6).

5.7 Placebo testing

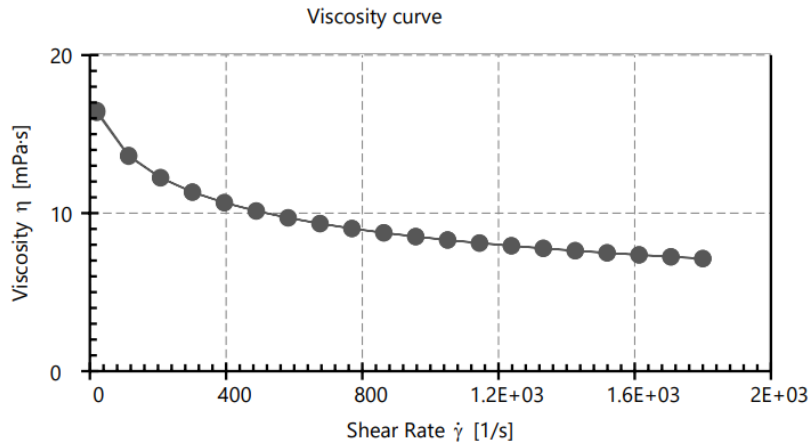
To improve the viscosity the obvious solution was to alter the Avicel concentration within the sample, as this excipient is responsible for giving the viscous properties to the product. Or better said, it is the sodium-carboxymethyl-cellulose (NaCMC) that contributes to the viscosity increase in the product. Currently, the formulation contains 10.5 – 11.5 w/w% NaCMC alongside the other Avicel ingredient, microcrystalline cellulose (MCC).

Throughout these formulation experiments, the NaCMC content was altered, and the viscosity of the placebo was measured with the standard method in the rheometer. It is important to mention that a proper recipe was not available for the mixing of the placebo, meaning that no stirring time or other conditions were given, despite which, the placebo was produced successfully. The viscosity curve for this standard placebo is presented below in graph 14.



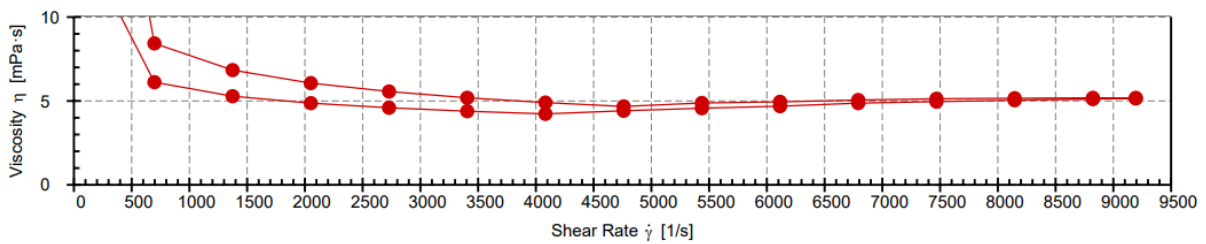
Graph 14. Showing the viscosity curve of the standard placebo, the viscosity value is 6,39 mPas.

Placebos were made with 22 w/w%, 15 w/w%, and 13 w/w% of NaCMC, respectively. For obvious reasons (as the product formulation is proprietary), the exact amounts of the various excipients are not shown in my thesis report, only the w/w% of NaCMC. The production of the 22 w/w% and 15 w/w% was not successful as lumps started to occur and it became impossible to dissolve the Avicel in the water. However, the 13 w/w% placebo was successfully made, and the viscosity has increased to 7,2 mPas, the viscosity curve for this formulation is presented in graph 15. below.



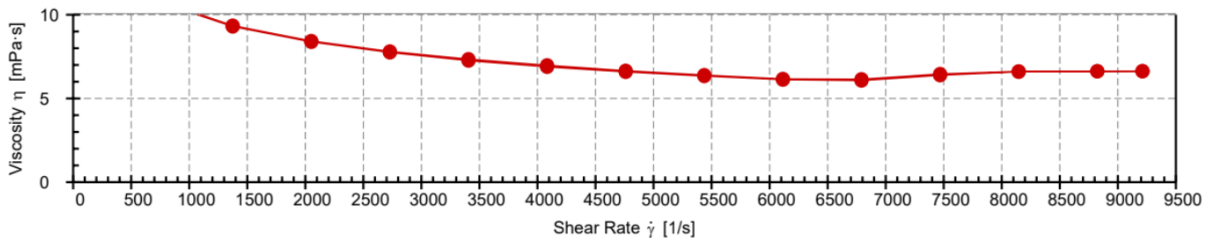
Graph 15. Showing the viscosity curve of the placebo containing 13 w/w% of NaCMC.

Also, for both the in-house standard placebo and the placebo containing 13 w/w% sodium-carboxymethyl-cellulose, the high shear rate curves were made and can be seen below in graph 16. and 17., respectively.



Graph 16. Showing the high shear viscosity curve of the standard placebo.

Graph 16. seen above represents the behaviour of the in-house standard placebo under high shear rate, the produced graph looks like the other standard curves. On the contrary, the upward and downward curves are barely distinguishable in graph 17. showing the response to a high shear rate in the sample containing 13 m/m% of NaCMC.



Graph 17. Showing the high shear viscosity curve of the placebo containing 13 w/w% of NaCMC.

6. Discussion

6.1 Investigation of temperature dependent viscosity

For investigating the temperature dependence of the product, the idea came from different scientific papers, that also included studies on Avicel. These articles suggested a decrease in viscosity with raised temperatures and an increase in this value by cooling [31], [32]. Also, it is a known fact that at higher temperatures the particles are moving around more quickly resulting in a decrease of viscosity as the time for particle-particle interactions shortens, as the distance increases between molecules [43].

As seen from the graph above (graph 5. and the graphs in Appendix 10.1), despite the supposed increase in viscosity due to lower temperatures, the conducted experiments did not back up this hypothesis. On the contrary, the opposite was true as higher viscosity values were seen in the samples held in warmer temperatures. The elevated temperature can contribute to faster dissolution of Avicel in the water, thus leading to an increased viscosity value in a shorter period.

Although keeping the samples at warmer conditions helped in the viscosity increase, the difference between these samples and the standard ones is in most cases only a 0.1- 0.2 mPas viscosity growth), thus this temperature change did not influence the viscosity to a high extent. Also, after seeing the same results in the second batch, and observing that cooling of the samples does not result in higher values, this was completely omitted from the temperature dependent viscosity measurement method.

What can also be seen from graph 5. is that the viscosity values on 30 °C roughly have only changed with the value of 0.26 mPas between day 2 and day 40 (viscosity value difference between day 0 and day 40 is 0,56 mPas), which raises the question if it is necessary to wait until day 6 or day 10 to measure? This same phenomenon was seen in the standard and cooled samples, as their value also barely changed between day 2 and day 30 (change in the viscosity value is only 0,24 mPas).

Also, it is important to mention that the viscosity of the product is already within the specification limit on day 0, meaning that the measurements can easily be taken on the day when the samples are received (this was seen in all other batches that are presented in the appendix). The specification limit is between 5,0 mPas to 8,5 mPas and as far as I know getting outside of specification for a sample has never happened before.

6.2 The influence of different shaking periods

By visually inspecting the product after the various shaking durations, clear differences were detected. On the bottom of the bottle that was measured at time zero, a clear white clump was seen, whilst the other bottles that were shaken seemed more homogenous. Also, it can be seen from the graphs (graph 6. above and the other graphs in Appendix 10.2) related to this measurement that the highest viscosity values were measured without any shaking (except in the first batch, this result is most likely due to batch-to-batch value deviation).

6.3 Test for thixotropic recovery

By measuring the samples after they have been standing in the Rheometer for an hour after being exposed to high shear, the results show that the one-hour waiting time is enough for the material to regenerate as the viscosity values barely vary from each other (can be examined from graph 7.). What can be read from the graphs (that are not presented in the thesis, but these values have been noted down) is that the initial viscosity from where the hysteresis loop starts decreases starting from the first measurement. But from our perspective what matters is the viscosity value quantified at the highest shear rate, and as said before, there are no deviations between the tests, thus the material seems to return to its original state in about an hour.

As the measurements showed almost the same results, the conclusion is that it takes less than an hour for the sample to return to its original structural state after high shearing. This means that the material is quite sturdy and resilient, thus when it gets filled into the bottles and stirred during mixing the viscosity goes back to the initial state maximum in an hour. This proves that the thixotropic characteristics cannot be held responsible for the slowly growing viscosity values between day 0 and day 10, meaning that there is something else that has an influence on the behavior of the material. This is most likely caused by not properly dissolving the Avicel in the initial step of the production, thus it takes days until the product reaches its state of equilibrium.

6.4 Frequency sweep and amplitude sweep

By conducting oscillating tests on the material, namely doing first an amplitude sweep, followed by a frequency sweep test, it can be determined if the material is likely to sediment or not. The amplitude sweep test (seen in graph 8.) provided information about the linear viscoelastic region and showed that the system starts to degrade after 10% of shear strain is reached.

In graph 9. (frequency sweep test) retrieved from the software, the loss, - the storage moduli and the complex viscosity are shown. By looking at the formation of these curves, we can detect a crossover between the G' and G'' curves, representing the sol-gel transition point. This means that, as the thixotropic gel (suspension) is sheared, the weak bonds are broken, and the material enters a liquid (sol) phase and is ready to be delivered to the nasal cavity. As seen, the complex viscosity is dependent on the frequency, comparing this received graph with data found in the literature [44], the system is likely to sediment.

Looking at the graphs generated from samples from batches no. 2, 3, and 4 (seen in Appendix 10.4), G'' curve is already positioned higher than the G' , meaning that even before the measurement starts, the material is already in the viscous liquid state. In batch no. 5 (found in Appendix 10.4) the sol-gel crossover is present. These differences can be explained by how the material was handled, as most likely for the samples that were distributed before the measurement the gel structure was broken.

6.5 High shear rate

To see the resistance of the material toward higher shear rates, this study was done. Inspecting the graph that was generated for batch no.1 (graph 10.) we can see that the material is extremely sturdy and resistant to mechanical stress, as for even relatively high shear rates the product still showed viscosity values that were within the specification.

Also, viscosity decrease can be examined as the shear stress starts to increase until a linear range is reached. According to the test method, the viscosity value is measured at $1740 \frac{1}{s}$, which is located at the beginning of this linear range.

In some regions, the viscosity decreases below 5,0 mPas (which is below the specification limit), but it is unlikely that the product gets subjected to such strong mechanical force. During transportation and if used as prescribed, the viscosity should be within the specifications.

An interesting phenomenon can be seen on the graphs in the appendix in batches no.2, 3, 4, and 5, as there seems to be a crossover point between the upwards and downward curve. This could mean that by a higher applied force, the behavior of the material switches from shear thinning to shear thickening. Also, the lowest points on the graphs mean that the maximum structural breakdown of the suspension has been reached, this in most cases means a viscosity value of 4.5 – 4.7 mPas at a shear rate of 4750 - 4080 $\frac{1}{s}$.

6.6 Particle size distribution

As this test gave information about the evenness and the uniformity of the product, it is important to look at the specifications presented above in section 8.6 according to the demands of the US market [42]. The goal was to gain knowledge about the different particle sizes by using the Spraytec equipment (from Malvern Instruments) to gain an understanding of the sedimentation process, as bigger particles have a higher tendency to sediment [14].

By looking at the results (graph 12.) it can be seen that the volume percentage of small particles fluctuates between 0.25 % and 0.75 % throughout the measuring days, thus this limit is met (limit is 6%). This is important since the small particles pose a severe health threat by traveling to the lungs [40]. The limit for the bigger particles, that are likely to get stuck in the throat (pharynx) [40] is also kept, as this is only between 0.3 % and 1.8 %, instead of 20%.

For the D values, the same is true as they must be in alignment with the specification limits. According to graph 13., D_{10} is between 19 μm and 21 μm , and the values for D_{50} are between 40 μm and 45 μm , thus these both meet the requirements. As for the D_{90} , the specification is 50 μm to 150 μm , thus this value is also within the limits (as it is always between 87 μm and 93 μm).

It is important to mention that there was no correlation found between the number of days passed and the particle size distribution. As the occurrence of big particles was not common, the conclusion is that the sedimentation is caused by not properly dissolved Avicel or by an oversaturated system. Also, the reason for the deviation between the different days was most likely caused by the bottle-to-bottle deviation and by the difference in the spray-head geometry.

6.7 Placebo testing

Creating the placebo has proven to be challenging as no proper recipe was available. The placebo containing 22 w/w% sodium-carboxymethyl-cellulose was not homogenous at all, as the self-made Avicel did not dissolve in the water, instead, it formed some bigger lumps. This was also examined at the 15 w/w% NaCMC placebo.

After further decreasing the NaCMC content, the 13 w/w% seemed to work as it produced a viscosity value of 7.2 mPas, in comparison to the in-house standard one (6.2 mPas). However, there were problems with this too, as soon as the stirring of the sample stopped, the sample started to settle and form a thick white layer at the bottom of the Erlenmeyer flask. This occurred as the system was most likely oversaturated. It is important to note that the sediment formation in the official product might also be caused by oversaturation.

Additionally, to the placebo mixing and viscosity measurements, the high shear curves were also made to see any difference to the standard product. The high shear rate curve (seen on graph 17.) of the 13 w/w% NaCMC containing placebo seemed odd, as there was hardly any difference between the up and down curve. Based on this curve, the product appears to be pseudoplastic and not thixotropic, but by looking at the report generated by the RheoCompass software the data showed a difference in the upwards and downward curves, thus it has proven that the product is thixotropic despite the odd look.

7. Conclusion

At this point, in the quality control laboratory, the viscosity measurement is the only test that cannot be done immediately after receiving the Rhinocort® samples (uniformity of dosage, pH, weighing and number of delivered doses, etc. can all be measured instantly). Although it can be quite stressful to measure everything on the same day, based on the experiments looking at the **temperature dependence of viscosity**, the opportunity is given to obtain the viscosity values already on day 0.

Also, if the aim is to get the highest value possible, keeping the samples at 30 °C and 75% relative humidity can lead to a faster viscosity increase in a shorter period. In the worst-case scenario, if the patients received the product on day 0 (which is highly doubtful) and kept it in the fridge (producing the lowest viscosity), the product would already be more than good for use as the viscosity of the sample is already within the specification on day 0 on all temperatures.

Throughout these experiments from **10 batches, 355 bottles** of Rhinocort® were examined. All measured viscosity values were within the specification limit on day 0, and only a slight increase was examined in the value on the following days. Consequently, my recommendation is to measure the viscosity of the product as soon as possible, which would significantly reduce storage costs, and would contribute to faster distribution.

As for the **shaking period**, my suggestion is to completely abandon this procedure altogether. The shaking of the samples leads to the destruction of structure and produces a lower viscosity value than the standard. Thus, after shaking, some time would be needed for the recovery.

This recovery has proven to take only for maximum an hour, as seen in the **thixotropic recovery** measurement, which meant that the thixotropic characteristic of the product cannot be held responsible for the slowly increasing viscosity value. The long waiting time is instead most likely caused by the oversaturation or by the not properly dissolved Avicel.

An additional concern was evaluated by the **amplitude, - and frequency sweep** tests, namely the likelihood of sediment formation. These tests confirmed that the product is likely to sediment from day 0, which should be taken into consideration in the production site, as the product should not be left in the pipes for too long to avoid handling difficulties.

The measurements executed on a **high shear rate** have shown that the product is highly robust, and its viscosity is fluctuating around 5,0 mPas no matter how high forces are applied, thus

meeting the specification limits. Also, it has given insight into the reason behind the setup of the test method, as the measurements are done at the beginning of the linear range in the viscosity curve.

Particle size distribution was examined to see if the size of the different particles contributes to sediment formation or not. Throughout these measurements, everything has proven to be in accordance with the specification limits, and no correlation could be found between the size of the particles, and the number of days passed.

Lastly, by producing **placebos** containing different w/w% of sodium-carboxymethyl-cellulose and examining their properties a higher viscosity value was achieved, but the sediment formation was present and most likely caused by oversaturation. Overall, I believe that the formulation of the product could be evaluated and tested on its own in a separate thesis work, although I see no need for such experiments as the product is within the specifications and works as it should.

8. Future work

Although some experiments were quite time-consuming, all preliminary set goals were reached throughout the thesis work. All results support the idea that the viscosity measurements can be done immediately after production, namely already on day 0. Measuring the time, - and temperature dependence of the product in 10 various batches was successfully achieved besides other experiments.

However, there is always more to be done as all these tests have to be validated and double-checked. As far as I know, the 2-hours shaking before measuring viscosity is already dismissed by the company, based on my measurements.

The most important experiments to be carried out in the future are further tests on several additional batches on day 0, to ensure that the viscosity is already adequate. Hopefully, these experiments will support my suggestions so that the testing on any day after production will be approved.

Additionally, if needed, the formulation of the product can be examined in the future as individual thesis work. With only a few experiments, I have only scraped the surface of the formulation, thus I would recommend looking into it to see if the system is oversaturated or if the Avicel is not properly dissolved in the initial step of the production. Furthermore, I would recommend a revision of the test method for the viscosity analysis as I believe the written text could be more precisely formulated.

I hope that my work will be useful in providing the opportunity to measure the viscosity as soon as possible and that all other experiments can be used as an indication of the robustness of the McNeil product, the Rhinocort®.

9. References

- [1] Medbroadcast, Rhinocort Aqua (budesonide nasal spray).
- [2] Johnson & Johnson, Rhinocort Aqua - budesonide.
- [3] G. Scadding, A. N. Greiner, P. W. Hellings, G. Rotiroti, and G. K. Scadding, Allergic rhinitis, *The Lancet*, vol. 378, pp. 2112–2122, 2011, doi: 10.1016/S0140.
- [4] J. Hellgren, A. Cervin, S. Nordling, A. Bergman, and L. O. Cardell, Allergic rhinitis and the common cold - High cost to society, *Allergy: European Journal of Allergy and Clinical Immunology*, vol. 65, no. 6, pp. 776–783, 2010, doi: 10.1111/j.1398-9995.2009.02269.x.
- [5] P. Small and H. Kim, Allergic rhinitis, *Allergy, Asthma & Clinical Immunology*, vol. 7, no. S1, p. S3, Dec. 2011, doi: 10.1186/1710-1492-7-S1-S3.
- [6] L. M. Wheatley and A. Togias, Clinical practice. Allergic rhinitis., *N Engl J Med*, vol. 372, no. 5, pp. 456–63, Jan. 2015, doi: 10.1056/NEJMcp1412282.
- [7] M. U. Ghori, M. H. Mahdi, A. M. Smith, and B. R. Conway, Nasal Drug Delivery Systems: An Overview, *Am J Pharmacol Sci*, vol. 3, no. 5, pp. 110–119, 2015, doi: 10.12691/ajps-3-5-2.
- [8] S. Appasaheb, S. D. Manohar, and R. Bhanudas, A Review on Intranasal Drug Delivery System, Maharashtra, India, 2013. [Online]. Available: www.japer.in
- [9] P. G. Djupesland, Nasal drug delivery devices: Characteristics and performance in a clinical perspective-a review, *Drug Delivery and Translational Research*, vol. 3, no. 1. Springer Verlag, pp. 42–62, Feb. 01, 2013. doi: 10.1007/s13346-012-0108-9.
- [10] H. A. Barnes, J. F. Hutton, and K. Walters, An Introduction to Rheology, *Elsevier Science Pub. Co*, 1989.
- [11] M. Aulton and K. Taylor, *Pharmaceutics The Design and Manufacture of Medicines*. 2018.
- [12] L. Newey-Keane and S. Carrington, Controlling the Stability of Medicinal Suspensions, *American Pharmaceutical Review*, Dec. 01, 2016.
- [13] S. S. Sangolkar, V. S. Adhao, D. G. Mundhe, and H. S. Sawarkar, Particle size determination of nasal drug delivery system: A review, 2012. [Online]. Available: www.globalresearchonline.net
- [14] Malvern Spraytec, 2017.
- [15] Malvern Instruments, A Basic Introduction to Rheology. 2016. Accessed: Jan. 21, 2023. [Online]. Available: www.malvern.com
- [16] J. Vlachopoulos, The Role of Rheology in Polymer Extrusion, 2003. [Online]. Available: <https://www.researchgate.net/publication/266472193>
- [17] EUROPEAN PHARMACOPOEIA 7.0.
- [18] EUROPEAN PHARMACOPOEIA 7.0 2.2.10. Viscosity-Rotating viscometer method.
- [19] V. S. Kulkarni and C. Shaw, Rheological Studies, in *Essential Chemistry for Formulators of Semisolid and Liquid Dosages*, Elsevier, 2016, pp. 145–182. doi: 10.1016/b978-0-12-801024-2.00009-1.
- [20] A. Sojoudi and S. C. Saha, Shear Thinning and Shear Thickening Non-Newtonian Confined Fluid Flow over Rotating Cylinder, *American Journal of Fluid Dynamics*, vol. 2, no. 6, pp. 117–121, Jan. 2013, doi: 10.5923/j.ajfd.20120206.04.
- [21] D. E. Alexander, Biological Materials Blur Boundaries, in *Nature's Machines*, Elsevier, 2017, pp. 99–120. doi: 10.1016/b978-0-12-804404-9.00004-9.

- [22] N. S. Yagnesh and K. R. Santosh, Pharmaceutical suspensions: Patient compliance oral dosage forms, *World J Pharm Pharm Sci*, vol. 5, no. 12, pp. 1471–1537, 2016, doi: 10.20959/wjpps201612-8159.
- [23] P. Rhinocort and M. Consumer Healthcare, PRODUCT MONOGRAPH INCLUDING PATIENT MEDICATION INFORMATION Budesonide Aqueous Nasal Spray 64 mcg per metered dose Corticosteroid for Nasal Use, 1997.
- [24] H. A. Barnes, Thixotropy a review, 1997.
- [25] J. Delegido, M. Dolz, M. J. Hernández, and J. Pellicer, Pseudoplasticity and thixotropy of different types of starch hydrogels prepared with micro crystalline cellulose-sodium carboxymethyl cellulose, *J Dispers Sci Technol*, vol. 16, no. 3–4, pp. 283–294, Apr. 1995, doi: 10.1080/01932699508943680.
- [26] M. Holtzapfle, Cellulose, *Texas A & M University, USA, Elvise Science Ltd.*, 2003.
- [27] D. Trache *et al.*, Microcrystalline cellulose: Isolation, characterization and bio-composites application—A review, *International Journal of Biological Macromolecules*, vol. 93. Elsevier B.V., pp. 789–804, Dec. 01, 2016. doi: 10.1016/j.ijbiomac.2016.09.056.
- [28] H. A. Ambjörnsson, K. Schenzel, and U. Germgård, CMC mercerization, 2013.
- [29] M. Dolz-Planas, C. Roldan-Garcia~, and J. v Herraiez-Dominguez’, Thixotropy of Different Concentrations of Microcrystalline Cellulose:Sodium Carboxymethyl Cellulose Gels BELDA-MAXIMINO’, 1990.
- [30] Y. Zhang, E. Tocce, H. Bertrand, and K. McIntyre, Polymer Influence on the Rheological Properties of Co-Processed Microcrystalline Cellulose and Sodium Carboxymethylcellulose, *Pharmaceutical Technology*, 2021.
- [31] S. C. Dhawale, S. G. Wadodkar, and A. K. Dorle, Behavior of suspending and wetting agents in aqueous environment, *Asian J Pharm*, vol. 3, no. 1, pp. 9–12, Jan. 2009, doi: 10.4103/0973-8398.49167.
- [32] M. Dolz-Planas, F. Gon~lez-Rodriguez, R. Belda-Maximino, and J. V Herraiez-Dominguez, Thixotropic Behavior of a Microcrystalline Cellulose - Sodium Carboxymethylcellulose Gel, 1988.
- [33] P. Kumar Verma, K. Arora, and V. Vats, Annals of Clinical Case Reports A Review on Pharmaceutical Suspension and Its Advancement, vol. 7, p. 2321, 2022, [Online]. Available: <http://anncaserep.com/>
- [34] T. George and M. F. Brady, Ethylenediaminetetraacetic Acid (EDTA), *StatPearls Publishing*, Jun. 2022.
- [35] Anton Paar, Basics of thixotropy.
- [36] G. Stojkov, Z. Niyazov, F. Picchioni, and R. K. Bose, Relationship between structure and rheology of hydrogels for various applications, *Gels*, vol. 7, no. 4. MDPI, Dec. 01, 2021. doi: 10.3390/gels7040255.
- [37] Azo Materials, Rheological Analysis of Dispersions by Frequency Sweep Testing, Jun. 06, 2005.
- [38] Malvern Instruments, Evaluation of the Dispersion Procedure, *Iodometric Assay - Antibiotics / Chemical Tests <429>*, 2016, doi: 10.6.1.1.
- [39] Malvern Instruments, Particle Sizing of Pharmaceutical Aerosols.
- [40] H. Hamishehkar, Y. Rahimpour, and Y. Javadzadeh, The Role of Carrier in Dry Powder Inhaler, in *Recent Advances in Novel Drug Carrier Systems*, InTech, 2012. doi: 10.5772/51209.

- [41] Consumer Healthcare McNeil, RHINOCORT® AQUA Corticosteroid for Nasal Use, 2017.
- [42] McNeil, US specification limits for particle size distribution in Rhinocort,
- [43] Z. Wenhao, Influence of Temperature and Concentration on Viscosity of Complex Fluids, in *Journal of Physics: Conference Series*, IOP Publishing Ltd, Jul. 2021. doi: 10.1088/1742-6596/1965/1/012064.
- [44] Malvern Instruments, Rheological analysis of dispersions by frequency sweep testing.

Table of figures

Figure 1. The product of McNeil is presented, 64 µg/dose Rhinocort® Aqua [picture taken on-site].	8
Figure 2. Showing the sensitisation process from DCs taking up the allergen to the symptom development by mast cell degranulation.	9
Figure 3. Representation of the main structures in the nasal cavity [7].	10
Figure 4. Two-plate model representing the shear stress and shear rate [10].	13
Figure 5. Representation of the capillary viscometer for measuring non-Newtonian fluid viscosity [17].	14
Figure 6. Shows the different geometries that are available for a rotational rheometer [19].	14
Figure 7. Showing the shear-thinning and shear-thickening behaviour in comparison to a Newtonian fluid [20].	15
Figure 8. Representation of thixotropic behaviour and formation of hysteresis loop [19].	16
Figure 9. Different regions found in natural cellulose [26].	17
Figure 10. Anton Paar MCR 302 with double-gap geometry in use [picture taken on-site].	19
Figure 11. Showing a frequency dependent system that is likely to sediment [37].	22
Figure 12. Presentation of the laser diffraction system with the different parts [13].	22
Figure 13. Showing the various D values and their meanings [14].	23

Table of graphs

Graph 1. Representing the method development for the high shear method.	25
Graph 2. Representation of the temperature dependence of the viscosity and inspection of a decrease in viscosity values by decreasing the temperature.	26
Graph 3. Representation of high temperature dependence of the viscosity, showing decrease or no change in the value.	26
Graph 4. Showing the three-interval test, starting from low shear, the second interval is the high shear, and the third interval is low shear again. The recovery percentage was not displayed.	27
Graph 5. Investigation of the temperature dependence of viscosity in the first batch, where the blue curve marks the cooled samples (6 °C), red curve shows the warmed bottles (30 °C), and the black curve shows the standard samples kept on room temperature (21 °C).	29
Graph 6. Representing the viscosity change due to various shaking periods.	30
Graph 7. Representing the time taken for full structural recovery, after the sample has been sheared.	31
Graph 8. Determination of the linear viscoelastic region.	32
Graph 9. Showing the behavior of the product and the tendency to sediment.	32
Graph 10. Presenting the viscosity curve up to 9500 1/s to examine the robustness of the product.	33
Graph 11. Showing the report made by the analyzing software. Some small particles can be examined, which are around 1 µm, the size for all other particles is between 10 – 100 µm.	34
Graph 12. Showing the volume present of particles of different sizes as the function of time (days).	35
Graph 13. Showing the size of different particles that can be found below the specific points on the particle size distribution graph as the function of time (days). These specific points being the D ₁₀ , D ₅₀ , and D ₉₀ .	35
Graph 14. Showing the viscosity curve of the standard placebo, viscosity value is 6,39 mPas.	36
Graph 15. Showing the viscosity curve of the placebo containing 13 w/w% of NaCMC.	37
Graph 16. Showing the high shear viscosity curve of the standard placebo.	37
Graph 17. Showing the high shear viscosity curve of the placebo containing 13 w/w% of NaCMC.	37
Graph 18. Representing the temperature dependence of viscosity in batch no. 2.	51
Graph 19. Representing the temperature dependence of viscosity in batch no. 3.	51
Graph 20. Representing the temperature dependence of viscosity in batch no. 4.	52
Graph 21. Representing the temperature dependence of viscosity in batch no. 5.	52
Graph 22. Representing the temperature dependence of viscosity in batch no. 6.	53

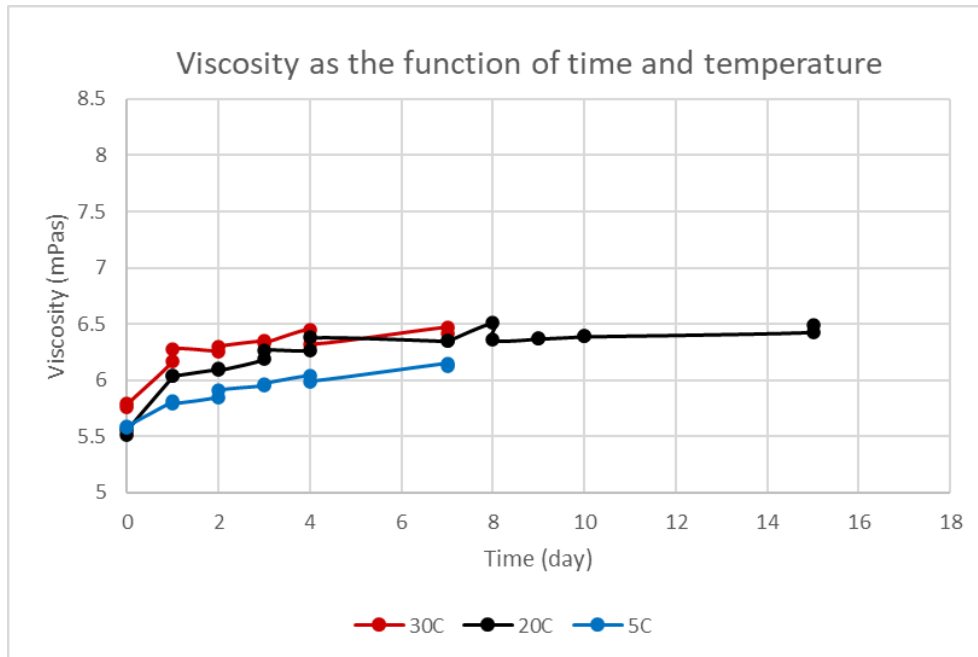
Graph 23. Representing the temperature dependence of viscosity in batch no. 7.....	53
Graph 24. Representing the temperature dependence of viscosity in batch no. 8.....	54
Graph 25. Representing the temperature dependence of viscosity in batch no. 9.....	54
Graph 26. Representing the temperature dependence of viscosity in batch no. 10.....	55
Graph 27. Displaying change in viscosity due to increased shaking period in batch no. 2.	55
Graph 28. Displaying change in viscosity due to increased shaking period in batch no. 3.	56
Graph 29. Displaying change in viscosity due to increased shaking period in batch no. 4.	56
Graph 30. Displaying change in viscosity due to increased shaking period in batch no. 5.	57
Graph 31. Showing the time taken for full thixotropic structural recovery in batch no. 2.....	57
Graph 32. Displaying the frequency sweep test for batch no. 2.	58
Graph 33. Displaying the frequency sweep test for batch no. 3.	58
Graph 34. Displaying the frequency sweep test for batch no. 4.	58
Graph 35. Displaying the frequency sweep test for batch no. 5.	59
Graph 36. Showing the behaviour of the nasal spray on high shear rate in batch no. 2.....	59
Graph 37. Showing the behaviour of the nasal spray on high shear rate in batch no. 3.....	59
Graph 38. Showing the behaviour of the nasal spray on high shear rate in batch no. 4.....	59
Graph 39. Showing the behaviour of the nasal spray on high shear rate in batch no. 5.....	60

Table of tables

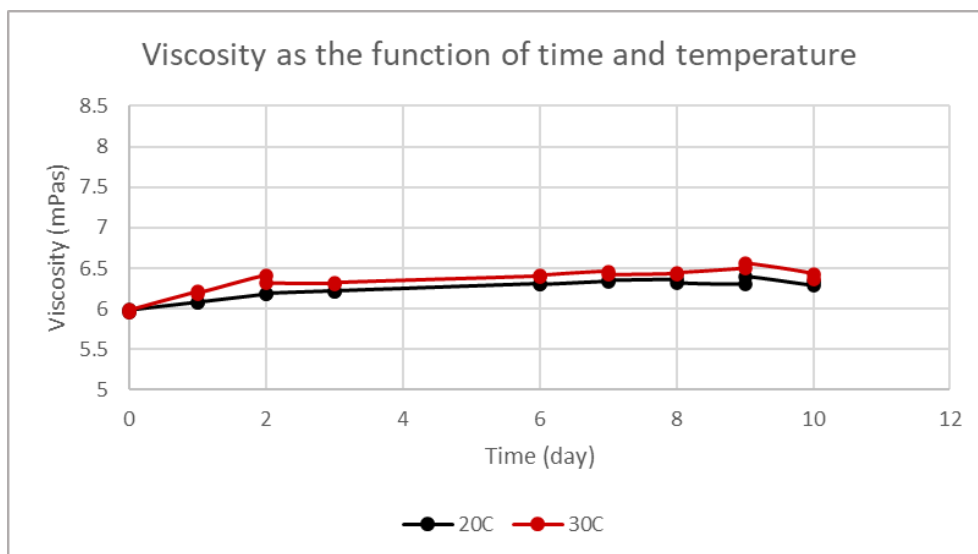
Table 1. Showing the important values from the report made by the analyzing software.....	34
-------------------------------------------------------------------------------------------	----

10. Appendix

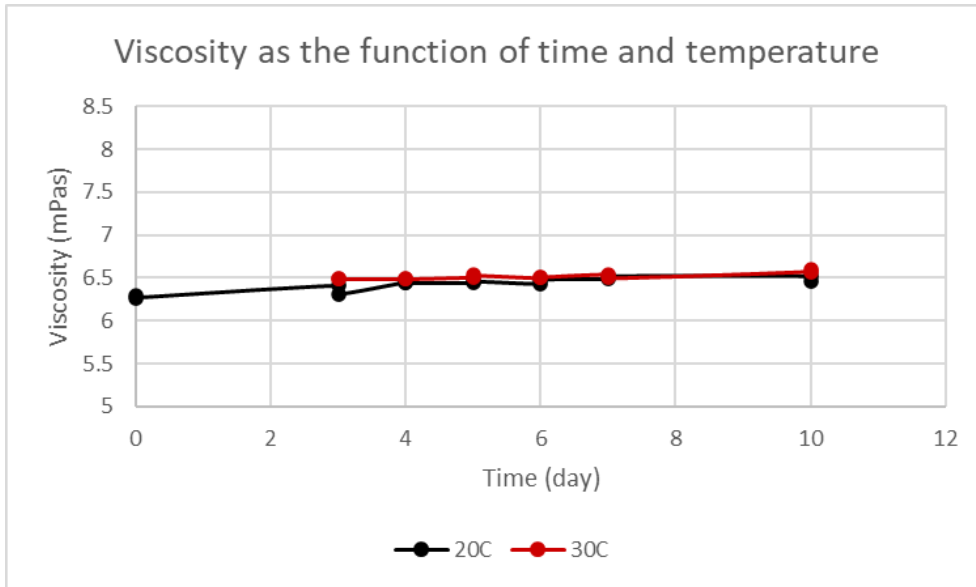
10.1 Temperature dependent viscosity



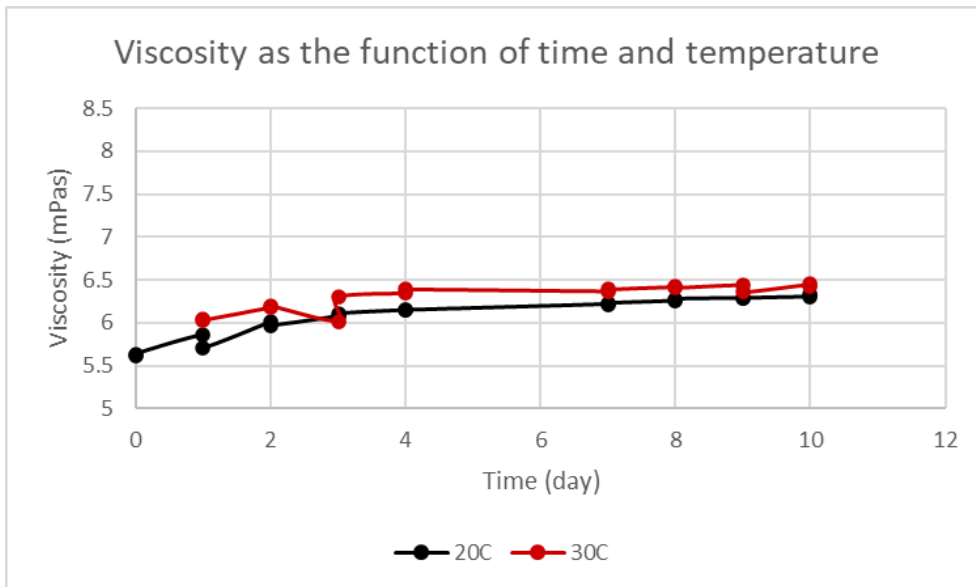
Graph 18. Representing the temperature dependence of viscosity in batch no. 2.



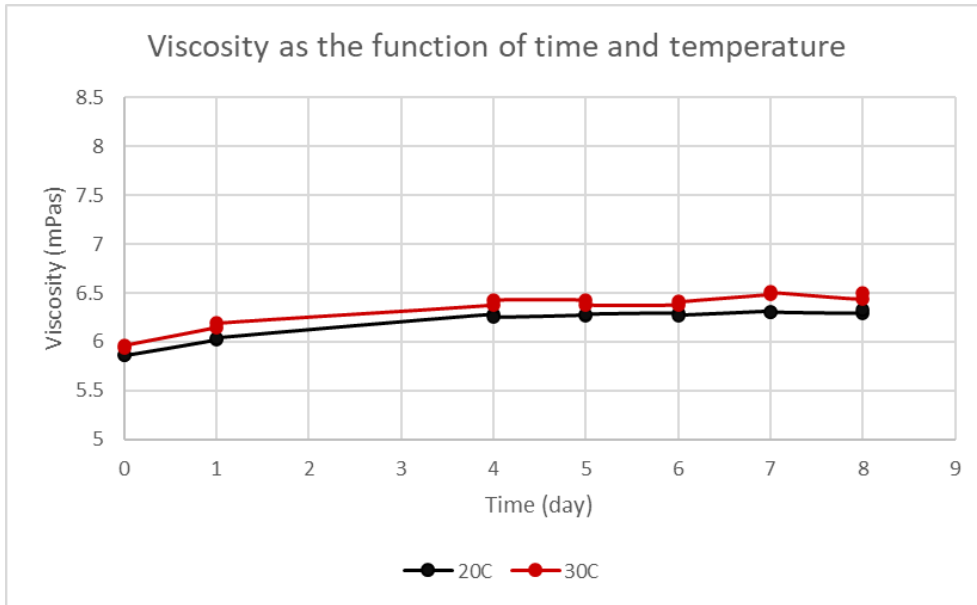
Graph 19. Representing the temperature dependence of viscosity in batch no. 3.



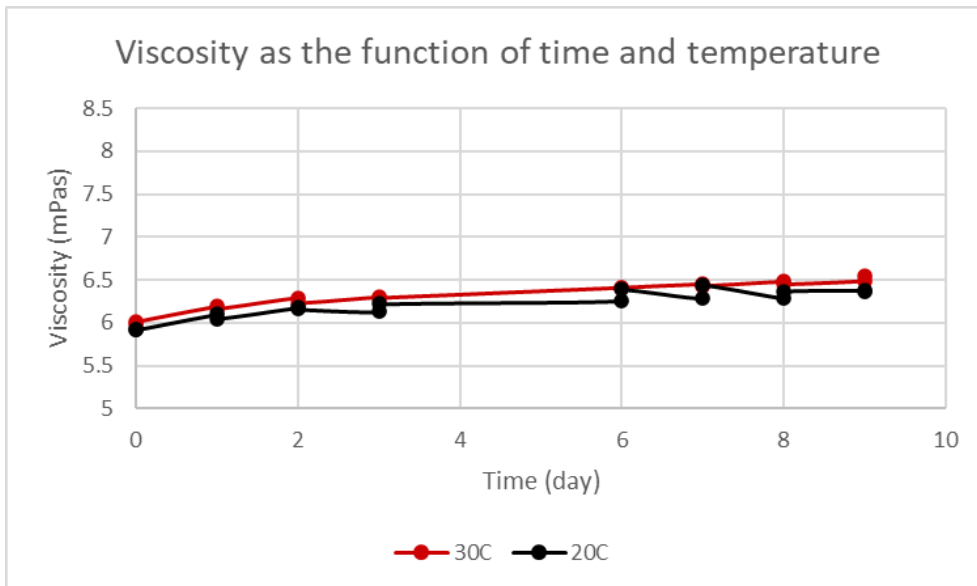
Graph 20. Representing the temperature dependence of viscosity in batch no. 4.



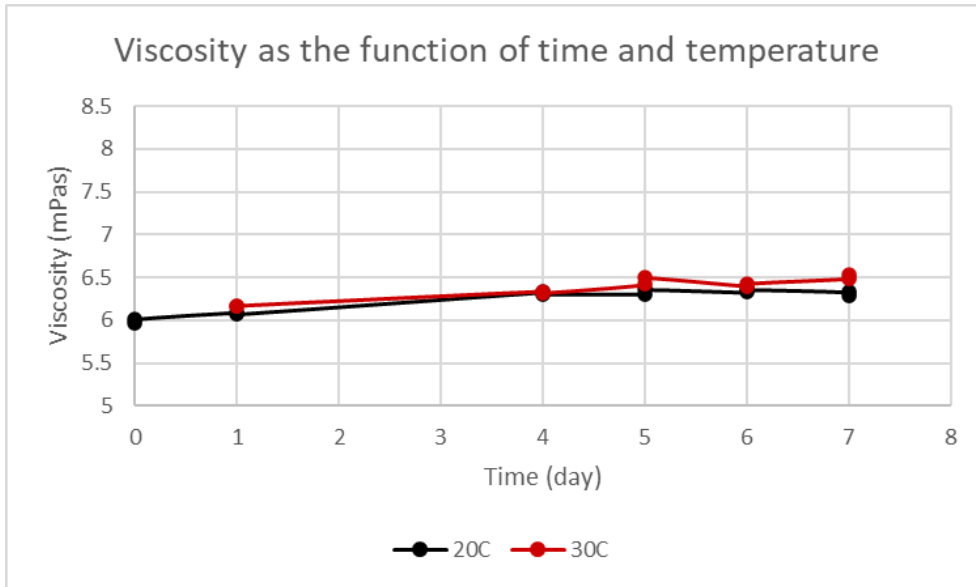
Graph 21. Representing the temperature dependence of viscosity in batch no. 5.



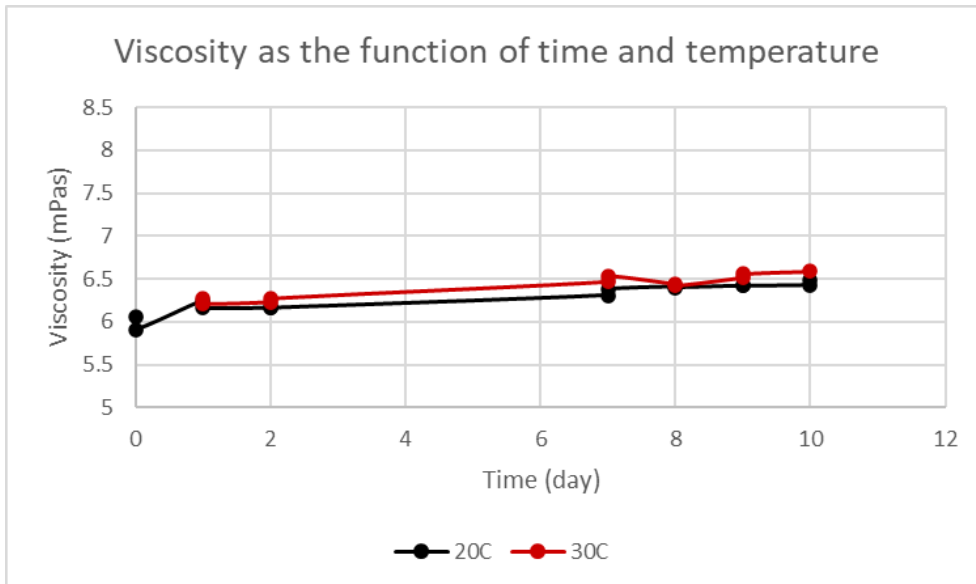
Graph 22. Representing the temperature dependence of viscosity in batch no. 6.



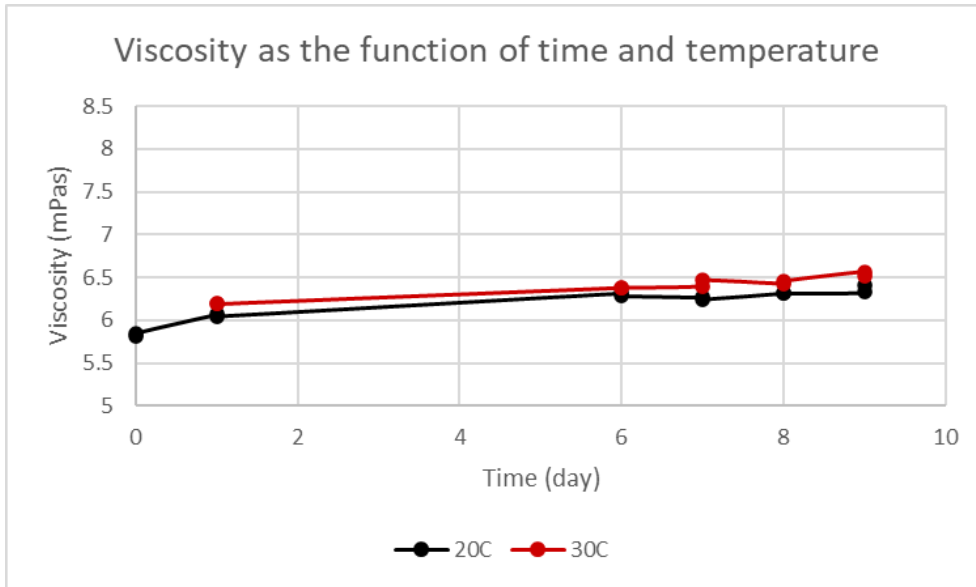
Graph 23. Representing the temperature dependence of viscosity in batch no. 7.



Graph 24. Representing the temperature dependence of viscosity in batch no. 8.

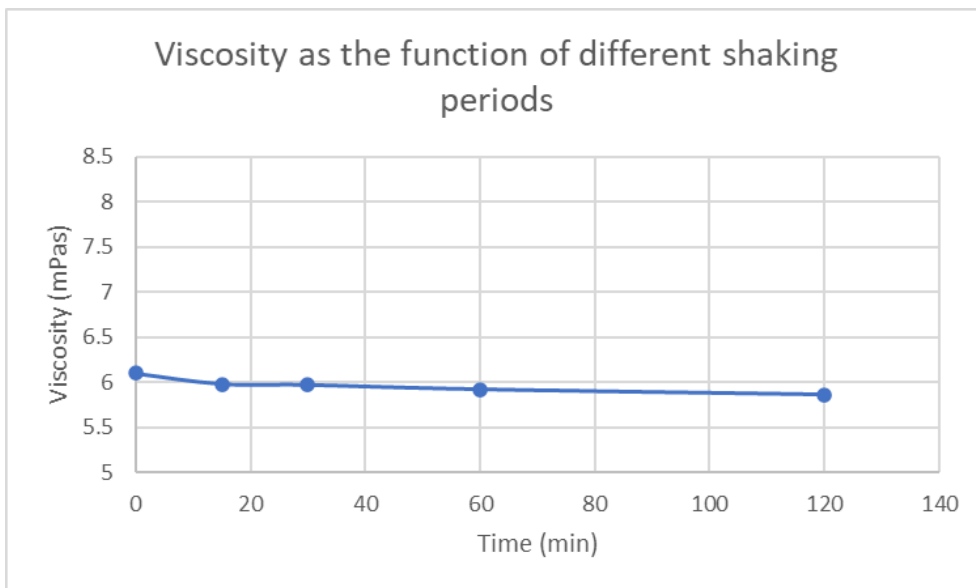


Graph 25. Representing the temperature dependence of viscosity in batch no. 9.

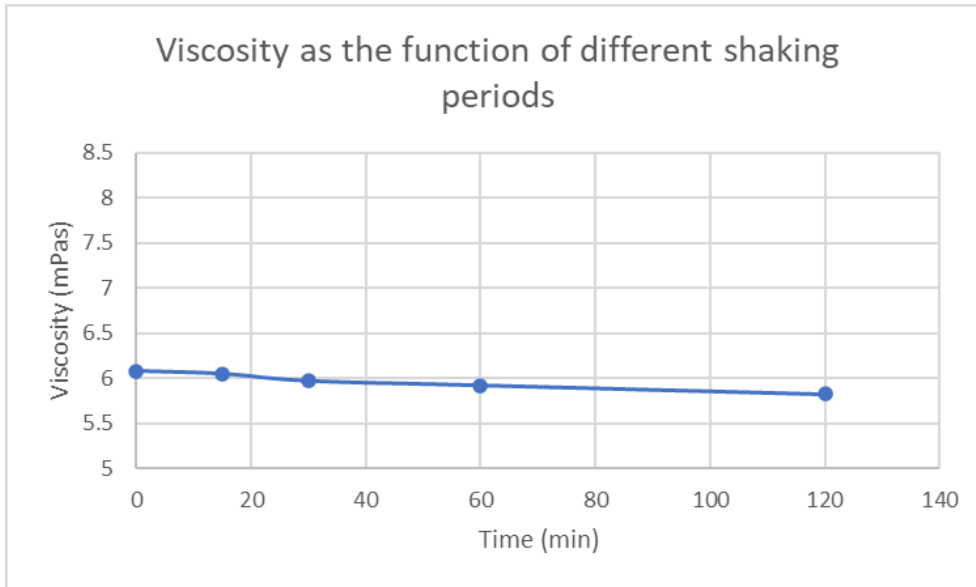


Graph 26. Representing the temperature dependence of viscosity in batch no. 10.

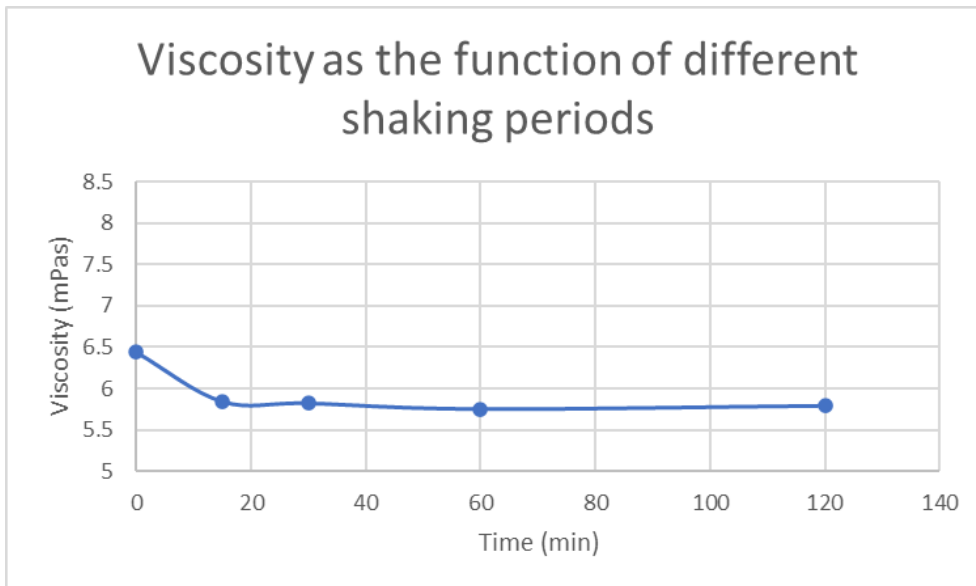
10.2 Viscosity as the function of various shaking times



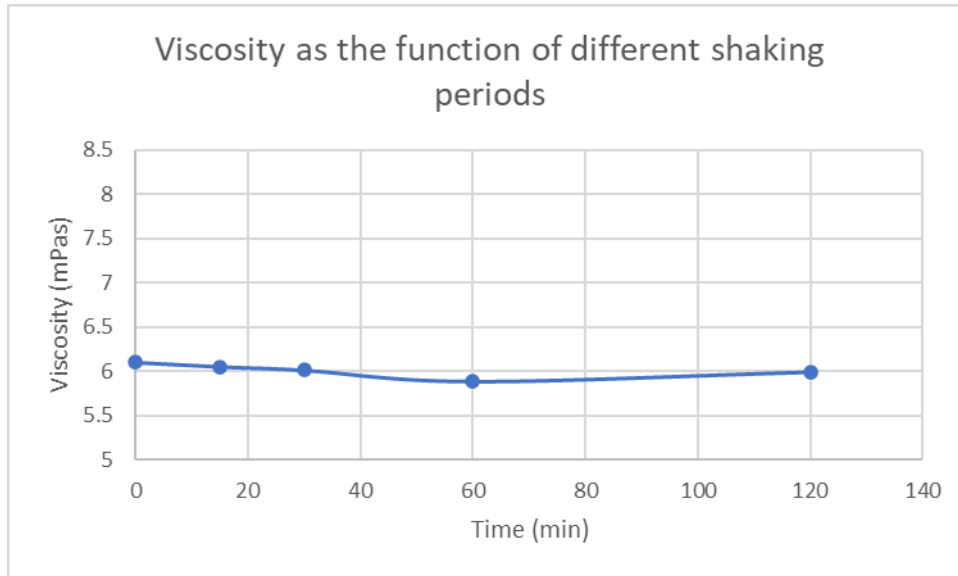
Graph 27. Displaying change in viscosity due to increased shaking period in batch no. 2.



Graph 28. Displaying change in viscosity due to increased shaking period in batch no. 3.

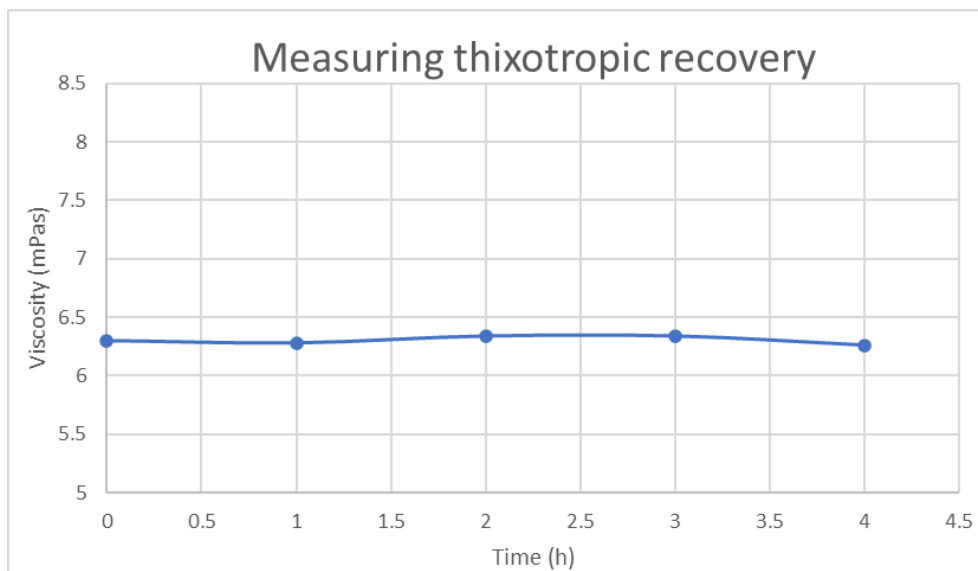


Graph 29. Displaying change in viscosity due to increased shaking period in batch no. 4.



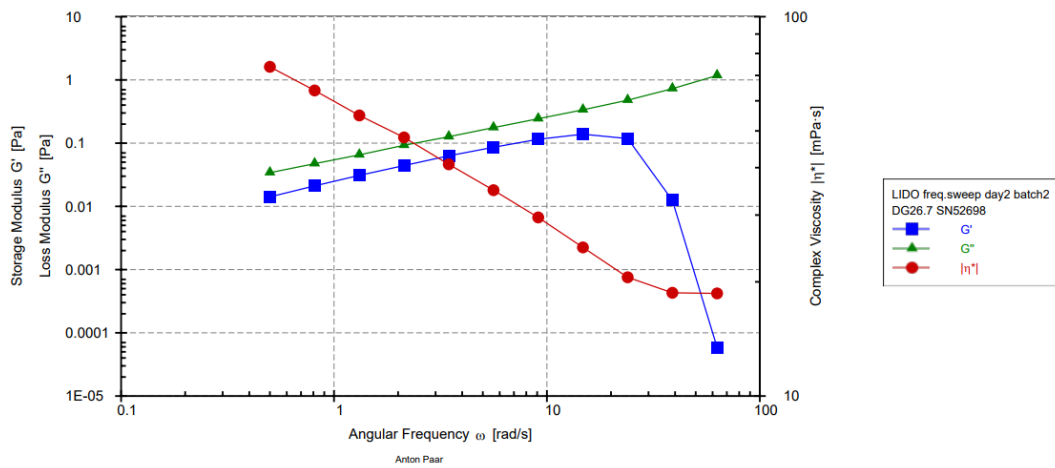
Graph 30. Displaying change in viscosity due to increased shaking period in batch no. 5.

10.3 Thixotropic recovery

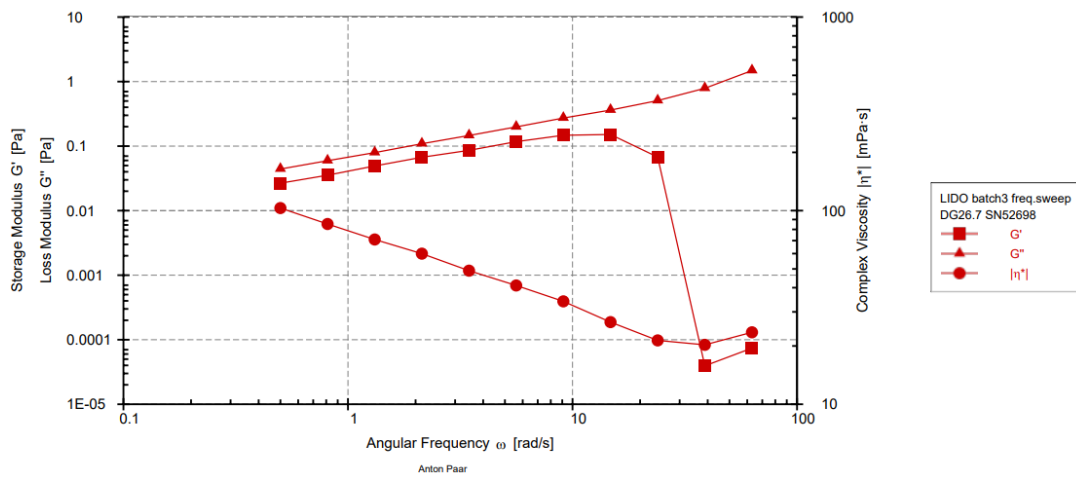


Graph 31. Showing the time taken for full thixotropic structural recovery in batch no. 2.

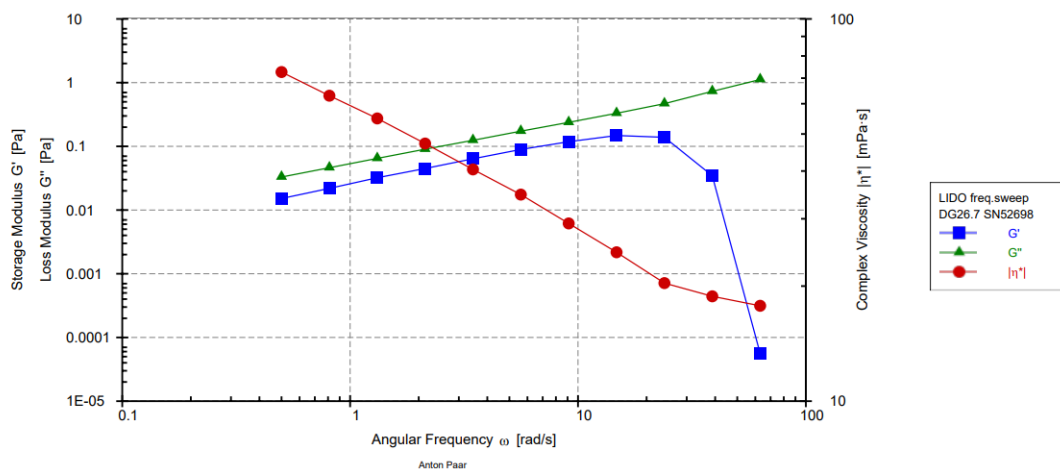
10.4 Frequency sweep



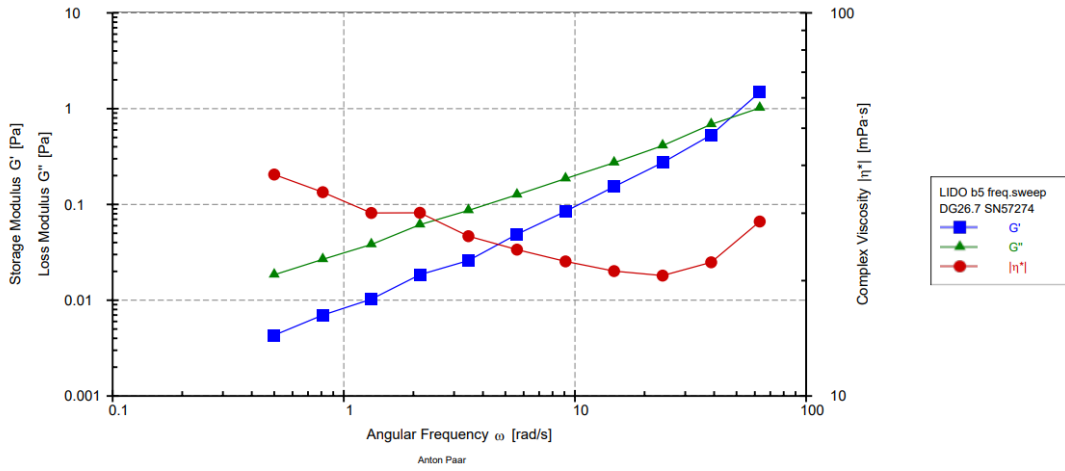
Graph 32. Displaying the frequency sweep test for batch no. 2.



Graph 33. Displaying the frequency sweep test for batch no. 3.

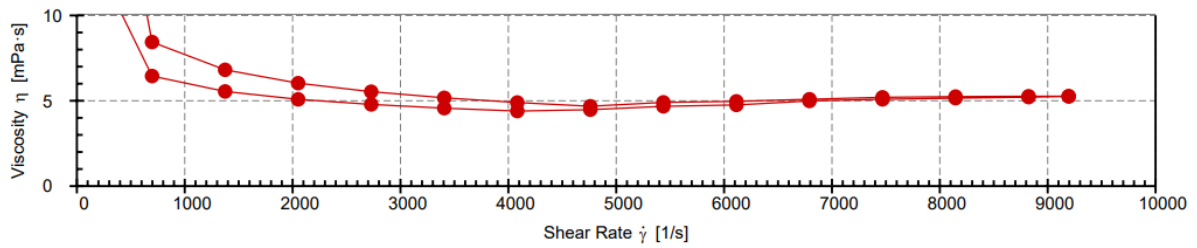


Graph 34. Displaying the frequency sweep test for batch no. 4.

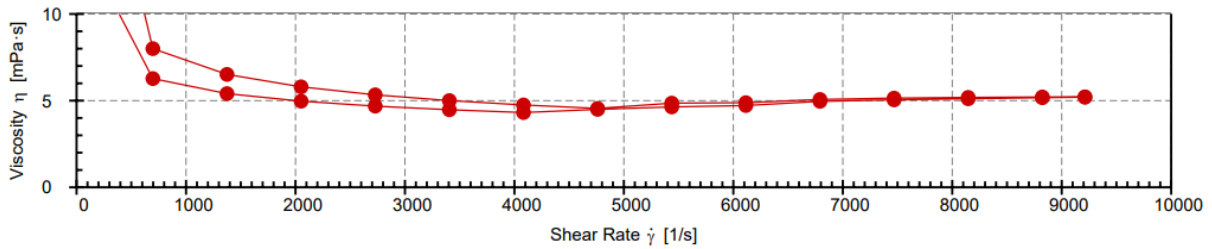


Graph 35. Displaying the frequency sweep test for batch no. 5.

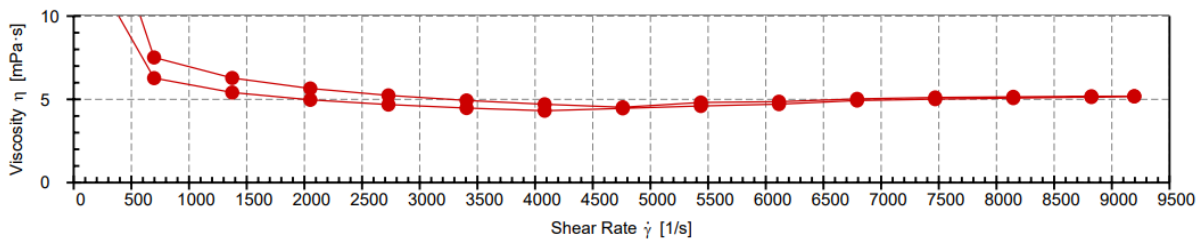
10.5 High shear



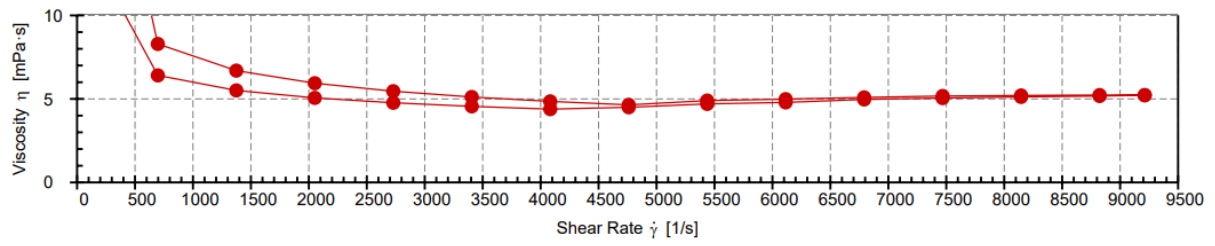
Graph 36. Showing the behaviour of the nasal spray on high shear rate in batch no. 2.



Graph 37. Showing the behaviour of the nasal spray on high shear rate in batch no. 3.



Graph 38. Showing the behaviour of the nasal spray on high shear rate in batch no. 4.



Graph 39. Showing the behaviour of the nasal spray on high shear rate in batch no. 5.